www.ceramsoc.com/en/

Available online at www.sciencedirect.com

ScienceDirect

J Materiomics 2 (2016) 1—24

www.journals.elsevier.com/journal-of-materiomics/

Lead-free piezoceramics — Where to move on?

Chang-Hyo Hong [a], Hwang-Pill Kim [a], Byung-Yul Choi [a], Hyoung-Su Han [a], Jae Sung Son [a], Chang Won Ahn [b], Wook Jo [a],*

[a] *School of Materials Science and Engineering, Ulsan National Institute of Science and Technology, Ulsan 44919, South Korea*
[b] *Department of Physics and EHSRC, University of Ulsan, Ulsan 44610, South Korea*

Received 11 November 2015; revised 11 December 2015; accepted 29 December 2015
Available online 21 January 2016

Abstract

Lead-free piezoceramics aiming at replacing the market-dominant lead-based ones have been extensively searched for more than a decade worldwide. Some noteworthy outcomes such as the advent of commercial products for certain applications have been reported, but the goal, *i.e.*, the invention of a lead-free piezocermic, the performance of which is equivalent or even superior to that of PZT-based piezoceramics, does not seem to be fulfilled yet. Nevertheless, the academic effort already seems to be culminated, waiting for a guideline to a future research direction. We believe that a driving force for a restoration of this research field needs to be found elsewhere, for example, intimate collaborations with related industries. For this to be effectively realized, it would be helpful for academic side to understand the interests and demands of the industry side as well as to provide the industry with new scientific insights that would eventually lead to new applications. Therefore, this review covers some of the issues that are to be studied further and deeper, so-to-speak, lessons from the history of piezoceramics, and some technical issues that could be useful in better understanding the industry demands. As well, the efforts made in the industry side will be briefly introduced for the academic people to catch up with the recent trends and to be guided for setting up their future research direction effectively.

Keywords: Lead-free piezoceramics; Doping effect; Incipient piezoelectricity; Piezoelectric applications

Contents

---

* Corresponding author.
E-mail address: wookjo@unist.ac.kr (W. Jo).
Peer review under responsibility of The Chinese Ceramic Society.

http://dx.doi.org/10.1016/j.jmat.2015.12.002

1. Introduction

More than 10 years of both extensive and intensive research activities have been devoted to developing lead-free piezoelectrics in response to the call for environmental protections [1−5]. From the beginning, the goal was obviously to develop lead-free piezoceramics whose properties are no less than those of the market-dominating lead zirconate titanate (PZT). At least when textured potassium sodium niobate (KNN)-based piezoceramics were reported by Saito et al. [6] in 2004, the goal appeared to be achievable quite readily [7]. Although most conceivable material systems have been explored and various strategies have been applied thereafter, the outcome does not seem so exciting as initially expected, given that lead-free piezoceramics are not yet the choice of materials for commercial products, though lead-free piezoceramics are introduced to selected commercial products [8]. Nevertheless, this does not mean that all the collective works by the community members are not noteworthy. In fact, a decade of worldwide research has led to the discovery of a number of potentially promising lead-free piezoceramics as well as valuable contributions to our better understanding of various phenomena in piezoceramics [7,9−21]. However, it is hard for one to deny the fact that scientific research activities are culminated [8], waiting for new issues. Hence, it is right time that we search for how to reactivate scientific research activities both inside and outside the community.

It is said that the relatively long history of piezoelectric community is indebted to the advent of several groundbreaking events such as the invention of $BaTiO_3$ [22] and $Pb(Zr,Ti)O_3$ (PZT) [23], the discovery of morphotropic phase boundary (MPB) [24−27], advanced understandings of relaxor ferroelectrics [28], doping effect based on the defect chemistry [29], and the utilization of polarization rotation in the relaxor-based single crystals [30,31]. As noted, each event has dedicated significantly to the growth of the community both in size and in quality, making the working concepts for developing new materials and applications. It is undeniable that the strategies and approaches taken for developing new lead-free piezoelectric materials are mostly rooted from them. However, it turns out that those concepts are not so efficient for lead-free piezoelectric materials as for lead-containing ones [9−17] Though not clear yet, two reasons could be considered for the unsatisfactory results during the transfer of those working concepts to developing lead-free piezoelectric materials. One possibility is that we might have missed some crucial considerations in establishing those working concepts, *e.g.*, the role of lead ion. Given that the MPB and the polarization rotation concepts have been developed inductively from the experimental observations in the lead-based piezoelectric materials [30,32], we cannot say that the applicability of the concepts onto the other material systems is guaranteed. In fact, there are a great amount of experimental results, the explanation of which does not fit into the classical theory. For example, many of MPBs identified in lead-free piezoceramics did not provide noticeable enhancements in piezoelectric properties like the conventional lead-based piezoceramics [33−40]. As well, the well-defined so-called ‘soft’ and ‘hard’ effects due to the presence of donors and acceptors, respectively, do not seem to be obvious in lead-free piezoceramics, especially the $(Bi_{1/2}Na_{1/2})TiO_3$ (BNT)-based ones [10,41−43]. For example, as will be discussed in a later section, none of the effects due to the presence of either acceptor or donor seems obvious in a number of lead-free piezoceramics in that the soft and hard effect represented by the increase in the electromechanical coupling factor and the mechanical quality factor, respectively, are, in principle, countereffective [44−48].

Apart from the scientific issues, scientific activities can also be significantly boosted up by bringing what has been achieved in the academia to the industry through technology transfers. Efforts in commercialization are sure to introduce new challenges, the solution of which requires further scientific insights. It is of course that scientific research activities to overcome these challenges will give rise to new applications for the industry. This means that the longevity and prosperity of the research field depend greatly on the establishment of this virtuous cycle leading to mutual benefits for both the scientific community and the industry. Here, one of the most important prerequisites is a continuous communication between academia and industry. We believe that this communication needs initiating from the academic side, because the motivation for the transition to lead-free piezoelectrics is rather weak on the industry side.

Given the aforementioned situations, it would be helpful to the piezoelectric community for us to present some information on the issues requiring further investigations and on the issues the industry people do care but scientific people often neglect. For this regard, we first review some historical moments briefly, since a complete review on history of piezoceramics is available in literature [49]. Then, our focus will be on some fundamental issues, *e.g.*, rationalization of doping effects, physical (practical) meaning of key properties from a different point of view. We also focus on some information to be considered for commercialization with respect to application-specific requirements. We hope that this brief review on the theoretical achievements we have made so far by reviewing the matters at different angles and on the information from the industry point of view contributes to a re-booming of the related research.

1.1. Historic events & challenges

Piezoelectric material is a dielectric material that enables a direct conversion between electrical and elastic energy. When subjected to an electric field, a piezoelectric material changes its dimension, and, conversely, generates a dielectric displacement in response to mechanical stress. The discovery of piezoelectricity dates back to 1880, when Curie brothers realized that an electrical charge was induced in a quartz crystal when pressure was applied. As demonstrated by Voigt in 1910 [50], this unique feature originates merely from a crystallographic consideration. This means that any crystal should exhibit piezoelectricity as long as it belongs to one of the 20 point groups lacking inversion symmetry. However, the effect was so weak in most known crystals that not many practical applications utilizing the piezoelectricity had been introduced.

A breakthrough in the development of piezoelectricity was made when barium titanate ferroelectric ceramic was discovered in 1940s. The importance of this finding is found in the fact that noticeably large piezoelectricity of a practical importance can be secured even in ceramic materials where a random orientation is unavoidable. Note that the symmetry constraint allows only single crystalline materials to exhibit piezoelectricity due to the unavoidable loss of macroscopic symmetry stemming from the random distribution in polycrystalline states. Thanks to the inherent feature of the ferroelectricity of barium titanate, which allows a reversal of polarity by the application of electric field, ceramics that are much cheaper and easier to fabricate than single crystals stepped into piezoelectric category. As discussed by Jaffe [51], the use of ferroelectric materials enables one to induce a unique polar axis into a macroscopically nonpolar ceramic through so-called poling process. As noted, the piezoelectric effect induced in this ferroelectric material was shown to be by far larger than the existing single crystal piezoelectrics. Naturally, this successful development of the first polycrystalline piezoelectrics inspired an extensive search for better piezoceramics, leading to the discovery of lead zirconate titanate (PZT) ceramic solid solutions in 1950s, which are still the most widely used piezoceramics with their exclusively excellent piezoelectric performances.

The discovery of PZT was a historic turning point to the piezoceramic community not only because of its excellent piezoelectric properties but also because of the birth of a new concept, so-to-speak, ‘morphotropic phase boundary (MPB). Jaffe et al. [24] observed that the electromechanical properties such as the radial electromechanical coupling coefficient (k_{31}) and the axial piezoelectric coefficients (d_{33}) peak when the composition of PZT approached a phase boundary between rhombohedral and tetragonal symmetry. This finding of an MPB-induced property enhancement has established a new paradigm in searching for new piezoceramics afterwards. In fact, the MPB-induced property enhancement in solid solution systems was already predictable from the studies of barium titanate, where piezoelectric properties peak whenever a phase transition so-called polymorphic phase transition (PPT) happens [52] such as from rhombohedral to orthorhombic and then to tetragonal and finally to cubic with increasing temperature [24,32,53–58]. Apart from the differences in the underlying mechanism for the property enhancement between MPB and PPT, an agreement was reached on the fact that a key to enhancing the piezoelectric properties is the coexistence of phases with different symmetries.

Since the discovery of PZT with an MPB as a working concept, the field of piezoceramics together with ferroelectrics has become one of the biggest research areas, opening up a huge world market with numerous applications [15,59]. In spite of the great success of PZT with the MPB concept, this MPB concept had failed in developing other material systems that surpass PZT with respect to piezoelectric properties had been made until 1997, when Park and Shrout [30] reported giant d_{33}' s of >2500 *pC/N* and huge electromechanical strains of ~1.7 % in $Pb(Zn_{1/3}Nb_{2/3})O_3$-$PbTiO_3$ (PZN-PT) and $Pb(Mg_{1/3}Nb_{2/3})O_3$-$PbTiO_3$ (PMN-PT), so-called relaxor-PT single crystals. More importantly from the practical point of view, what was noted is that unexpectedly, this extremely high functional properties were available not at the MPB but at the rhombohedral side of MPB. As well, the best properties were obtained in ⟨001⟩-oriented rhombohedral crystals though the polarization direction of rhombohedral crystals is [111]. It is no wonder that these unexpected findings soon led to another boom in piezoelectric research activities both theoretically and practically, replacing the original idea on the MPB, stating that the coexistence of different phases leads to an increase in the multiplicity of possible poling directions [32] with a new one based on the polarization rotation concept dictating an easier polarization rotation near a MPB [60].

Although this newly proposed MPB concept has been accepted quite widely, it seems that it still lacks clarity. Soon after Park and Shrout [30], Fu and Cohen [61] showed by a first principles calculation on a model barium titanate system at the absolute zero that the polarization rotation could be indeed a true mechanism for the experimentally observed ultrahigh electromechanical responses of the single crystalline PZN-PT and PMN-PT, emphasizing that the effect should be valid only in single crystals due to the orientational randomness inherent to polycrystals. The effect of polarization rotation was also confirmed to be valid in BT [62], but it was, indeed, recently shown in BNT-BT system that the polarization rotation itself does not seem to be effective in enhancing piezoelectric properties of ceramics [63]. On the other hand, inspired by the proposed polarization rotation mechanism stating that the polarization rotation path involves monoclinic symmetry, several research groups reported that the alleged rhombohedral and tetragonal mixture in MPB region should actually be a monoclinic symmetry [64–74], which is contradictory to the term MPB itself, *i.e.*, MPB requires more than two phases. Though the existence of monoclinicity at MPB is still controversial [68,75,76], Cohen's group, who initially claimed that the polarization rotation concept should be ineffective in polycrystalline materials, proposed that the monoclinicity itself guarantees the enhanced electromechanical properties even in polycrystalline materials. The existence of monoclinicity was proposed to be a consequence of a chemical pressure exerted by the presence of Zr in $PbTiO_3$ lattice that has a monoclinic phase as a high pressure polymorph [27]. However, given that the proposed model faces a number of criticisms [77–84], it is said that the true origin of MPB is still unresolved.

1.2. Typical strategies for developing lead-free piezoceramics so far

As briefly discussed in the previous section, the research activities in the piezoceramic community has been driven by several important topics such as polymorphic phase boundary (PPB), and MPB. As expected, these two concepts have been extensively utilized in the study of lead-free piezoceramics. Among the two widely studied classes of lead-free piezoceramics are KNN- and BNT-based materials. Though the term, MPB, has been frequently cited in the study of BNT-based materials, the designation of this term is controversial because of the relaxor nature of BNT system. Given that this topic will appear again in the later sections, this section presents a brief review on how PPB and MPB concepts have been implemented in KNN-based piezoceramics.

1.2.1. T_{O-T} engineering

KNN is a solid solution between the ferroelectric KN with an orthorhombic symmetry and the antiferroelectric NN with another orthorhombic symmetry [18,21,85]. Different from PZT, the phase diagram of KNN is very complicated with three vertical MPB's between two different ferroelectric orthorhombic phases [86]. Among them, the one with ~50 at% K is of a common interest. Although KNN is featured by a fairly high Curie temperature at ~420 °C, it has comparatively poor piezoelectric properties at room temperature. It was reported that d_{33} and k_{33}^2 of hot-pressed dense samples are at most ~160 *pC/N* and ~0.3, respectively [87]. Therefore, most early studies have focused on how to enhance these functional properties through chemical modifications. A success, represented by Saito et al.'s work, has been made when the chemical modifications brings the T_{O-T} down to room temperature [18,33,34,88–112]. These enhanced functional properties are commonly called 'PPB' effect. However, this success has left a big challenge of how to secure the temperature stability of the enhanced properties without hampering them, because this PPB effect exists only in a narrow temperature range. Recently, Wang et al. [113] reported a sort of a partial success that for specific applications driven by a relatively high field, *e.g.*, 2 kV/mm, the temperature stability of the strain properties can be greatly enhanced by making PPB diffused through a chemical modification. It means that the this approach has its weakness to be a general solution that guides how to enhance functional properties for normal applications driven by a small electric field, *i.e.*, $\ll E_C$ by PPB engineering.

As discussed in the introduction, there is often a gap between what the academia pursues and what the industry demands. For example, academic people tend to aim for how to enhance properties either by chemical modifications or by modified processing routes. It is of course that the materials with excellent functional properties are also desired by the industry people, but this factor alone cannot qualify for commercialization. One of the important considerations is the temperature stability of those functional properties, the range of which depends on the type of applications, even though the temperature stability can only be secured at the expense of a degradation of those properties. In this sense, the T_{O-T} engineering needs approaching at a slightly different angle. It is well-acknowledged that the Curie temperature is one of the most important parameters to be considered for practical applications. For this regard, KNN may be considered a highly suitable for practical applications with its fairly high Curie temperature at 420 °C. However, this advantage becomes colorless due to the presence of another phase transformation from an orthorhombic to a tetragonal symmetry at ~200 °C, which replaces the Curie temperature for the practical criterion. For this reason, how to deal with T_{O-T} properly has been the research topic. Bringing T_{O-T} down below the lower-temperature limit for practical applications keeping the Curie temperature and the functional properties as high as possible would be the ideal option. Recently, Zhang et al. [114] reported a highly interesting result that the addition of $CaTiO_3$ into a KNN with T_{O-T} near room temperature enables a further shift of T_{O-T} down to 50 °C, while keeping the Curie temperature at as high as ~300 °C. Considering that one of the harshest temperature requirements for piezoceramics is −40–150 °C (a requirement enforced by automobile applications), this outcome is highly inspiring. Nevertheless, a catch is that this expenditure of the stable temperature range degrades the piezoelectric properties significantly, which offers room for further investigations, though some notable works have been reported [102,115,116].

1.2.2. Symmetry engineering

While most studies have focused on the PPB engineering, there have been some efforts to realize the PZT-like MPB in KNN-based piezoceramics, *i.e.* rhombohedral *vs.* tetragonal phase boundary. A core idea behind this is to bring lowest-temperature rhombohedral phase in KNN to room temperature. Wang et al. [117] demonstrated that the addition of $BaZrO_3$ serves this purpose right. This work has been followed by others [118,119], giving a rise to an empirical conclusion that Zr^{4+} seems to play an important role. These works confirmed that PZT-like 'MPB' can be, indeed, constructable in

KNN-based materials. However, this induced ‘MPB’ is presumably slanted in the temperature *vs.* composition phase diagram. This means that this ‘MPB’ is more like ‘PPB’ between rhombohedral and tetragonal, though this violates the group−subgroup relationship. The outcomes of the related research are listed in Table 1 [118−133]. To better formulate truly PZT-like MPB in KNN, *i.e.*, a vertical MPB between rhombohedral and tetragonal, further studies have been carried out based on an idea that strengthening rhombohedral ‘field’ in the PZT-like ‘MPB’ compositions would allow the existing rhombohedral symmetry to be more thermally-stable [119]. Though the idea appears simple, it seems quite working in that the MPB existing at room temperature persists up to ~250 °C with fairly good functional properties. Nevertheless, the extension of this MPB needs verifying below room temperature at least down to −40 °C.

2. Fundamental issues

2.1. Properties of a common interest

As noted, there are various properties that constitute the figure of merit of piezoelectric materials for certain applications [8]. The material constants most commonly referred to are electromechanical coupling factor, mechanical quality factor, and piezoelectric charge/voltage coefficient. The application of piezoelectric materials is usually categorized into four fields, *i.e.*, actuators, transducers, sensors, and generators. As will be later discussed, each application requires different properties depending on the design and the working conditions of devices. Therefore, it is useful for one to consider at least the target applications from the beginning. Given that the definition and description of each parameter are easily referenced in a number of textbooks, this review will focus mostly on the meaning of the electromechanical coupling and mechanical quality factor in terms of their physical and practical meaning.

2.1.1. Electromechanical coupling factor

What features the piezoelectricity is the presence of a coupling between electrical and mechanical energy. This means that a necessary and sufficient condition for a material to exhibit piezoelectricity is the presence of electromechanical coupling. The parameter that best-quantifies the coupling of piezoelectric materials is the electromechanical coupling factor, denoted as k^2. The physical meaning of the electromechanical coupling coefficient is the ratio of the mechanical energy stored due to piezoelectric effect to the electrical input energy or *vice versa*. Since piezoelectric materials are mechanical vibrators, the vibrating frequencies result in resonances defined by the given sample geometry. For the real applications, one adjusts the geometry in a way to utilize a single vibration mode. This means that the commonly cited electromechanical coupling factor can be understood as the maximum possible value at a given vibration mode.

We take the stored electrical energy as W^T with the application of an electric field when a material vibrates freely along a certain mode, *i.e.*, the capacitance of the material increases. As well, we designate the stored energy as W^S when the material is mechanically clamped in a way that no vibration is allowed, *i.e.*, the capacitance remains constant. The electromechanical coupling factor (k^2) is defined as

$$k^2 = \frac{W^T - W^S}{W^T} = \frac{\varepsilon^T E^2 - \varepsilon^S E^2}{\varepsilon^T E^2} = \frac{\varepsilon^T - \varepsilon^S}{\varepsilon^T}. \tag{1}$$

Therefore, we can understand k^2 as the portion of energy that is stored mechanically due to piezoelectric effect, since $W^T - W^S$ is the energy stored additionally due to a mechanical deformation.

For an illustration purpose, let us think of an imaginary plate-type piezoceramic cantilever where one dimension (x_1) is by far larger than the other two dimensions (along x_2 & x_3) so that we can assume that it only expands and shrinks along the largest dimension, *i.e.*, length mode vibration (Fig. 1). In this case, all the mechanical strain components and electric field components become trivial except for the mechanical strain component ($//x_1$) and electric field component ($//x_3$). Then, the strain (S) and the dielectric displacement (D) are given from the fundamental equations, $S_{ij} = s^E_{ijkl}T_{kl} + d_{kij}E_k$, and $D_i = d_{ikl}T_{kl} + \varepsilon^T_{ik}E_k$, as

$$S_1 = s^E_{11}T_1 + d_{31}E_3, \tag{2}$$

and

$$D_3 = d_{31}T_1 + \varepsilon^T_{33}E_3, \tag{3}$$

where S^E and d refer to elastic compliance in a short circuit condition and piezoelectric charge constant, respectively. Putting Eq. (2) into Eq. (3) with S_1 set to zero, Eq. (3) becomes

$$D_3 = d_{31}\left(-d_{31}E_3/s^E_{11}\right) + \varepsilon^T_{33}E_3 = \left(\varepsilon^T_{33} - d^2_{31}/s^E_{11}\right)E_3. \tag{4}$$

From an another fundamental equation, $E_i = -h_{ikl}S_{kl} + \beta^S_{ik}D_k$, we obtain

$$D_3 = E_3/\beta^s_{33} = \varepsilon^s_{33}E_3 \tag{5}$$

for $S_1 = 0$. The comparison of Eq. (4) and Eq. (5) yields a useful relation

$$\varepsilon^s_{33} = \varepsilon^T_{33} - d_{31}/S^E_{11}. \tag{6}$$

By putting Eq. (6) into Eq. (1), we obtain a very important relation between the electromechanical coupling factor and piezoelectric charge constant as

$$k^2_{31} = \frac{d^2_{31}}{\varepsilon^T_{33}s^E_{11}}. \tag{7}$$

In practice, this electromechanical coupling factor is commonly evaluated using a so-called resonance and anti-resonance technique. With increasing measurement frequency, the impedance of piezoelectric materials is typically revealed as shown in Fig. 2(a) due to a mechanical resonance, the frequency of which is determined by the sample geometry for a given vibration mode. The first peak, where the impedance becomes lowest, results from a resonance between the serially-connected mechanically-equivalent inductor (mass, denoted as L) and mechanically-equivalent capacitor (elastic compliance, denoted as C_1), as schematically shown in Fig. 2(b) [134]. This happens because L tends to get bigger with increasing frequency due to self-inductance in AC, while C_1 does the opposite, when they are serially-connected. This means that beyond this resonance frequency, the L component dominates and will resonate with the parallelly-connected electrical capacitor, C_0 with a further increase in the frequency, which is called the antiresonance (also called the parallel resonance). Note that the frequency dependence of L and C becomes opposite when they are connected parallel. The region bound by two frequencies, i.e., resonance and antiresonance, where the inductance dominates, is called the area of operation for a given vibration mode, meaning that the properties of piezoelectric vibrators comes from mechanically-equivalent inductance. Therefore, an ideal piezoelectric material exhibits a total phase angle change of 180° (−90° of pure capacitor to 90° of pure inductor and then to −90° of pure capacitor) during resonance and antiresonance with increasing frequency. This is one of the reasons why the phase angle change is often used to estimate the degree of poling.

Now, applying this concept to Eq. (1) to calculate, we get

$$k_{31}^2 = \frac{\varepsilon_{33}^T - \varepsilon_{33}^S}{\varepsilon_{33}^T} = \frac{C_0 + C_1 - C_0}{C_0 + C_1} = \frac{1}{1 + C_0/C_1}. \tag{8}$$

Here, C_0/C_1 is usually denoted as r, called capacitance ratio, which is considered to be one of the most important in practice, because it determines the sensitivity of resonance frequency to the changes in external circuit parameters. Given that the serial-resonance or resonance (f_s) and parallel-resonance or antiresonance frequency (f_p) is expressed as

$$f_s = \frac{1}{2\pi\sqrt{LC}}, \text{ and}$$

$$f_p = \frac{1}{2\pi\sqrt{L\frac{C_0C_1}{C_0+C_1}}} = \frac{1}{2\pi\sqrt{LC_1}}\sqrt{1+\frac{1}{r}},$$

rearranging the two equations yields

$$r = \frac{f_s^2}{f_p^2 - f_s^2}. \tag{9}$$

Putting Eq. (9) into Eq. (8) gives

$$k_{31}^2 = \frac{f_p^2 - f_s^2}{f_P^2}. \tag{10}$$

This means that the higher the antiresonance frequency and the larger the distance between the resonance and antiresonance frequency, the larger the electromechanical coupling factor.

Table 1
A variety composition and properties of lead-free piezoceramics.

Year	Compostion	Phase[a]	T_c	d_{33}	k_p	Ref.
2009	$(1-x)$KNN-xBZ, (x = 0−0.25)	R ($0.08 \le x \le 0.15$)	RT $\le T_c \le$ 200	–	–	[117]
2011	$(1-x)$KNN-xCZ, (x = 0.03−0.09)	O & R ($0.04 \le x \le 0.08$), R ($0.09 \le x$)	100 $_3$ 300	154 (x = 0.04)	32.2	[118]
2011	$(1-x)$KNBNZ-xLS, (x = 0.01−0.09)	O & R or R & T (x = 0.06), R ($0.07 \le x$)	80 $\le T_c \le$ 200	344 (x = 0.04)	32.4	[120]
2011	$(1-x)$KNN-xAZ, (A = Sr, Ca; x = 0−0.25)	Sr; R ($0.08 \le x \le 0.10$) Ca; R ($0.08 \le x \le 0.15$)	Sr; 120 $\le T_c \le$ 175, Ca; 120 $\le T_c \le$ 200	–	–	[121]
2011	$(1-x)$KNNS-xBNT, (x = 0−0.07)	R ($x \le 0.07$)	200	–	–	[122]
2011	0.92KNNS-(0.08-x)LT-xBZ, (x = 0−0.08)	R & T ($0.02 \le x \le 0.03$) R ($0.03 \le x$)	RT $\le T_c \le$ 220,	365 (x = 0.025)	45	[123]
2013	$(1-x-y)$BZ-xKNLN-yBNT	Vertical MPB; R & T (x = 0.915, y = 0.01)	270	285	42	[119]
2013	(0.974-x)KNN-0.026BKTxSZ3, (x = 0−0.07)	R & T (x = 0.05), R ($0.06 \le x$)	150 $\le T_c \le$ 200	324 (x = 0.05)	41	[124]
2013	$(1-x)$KNNT-xBZ, (x = 0−0.08)	O & R ($0.05 \le x \le 0.07$), R ($0.07 \le x$)	199 $\le T_c \le$ 240	193 (x = 0.06)	32.6	[125]
2014	$(1-x)$KNNL-xBZ, (x = 0−0.12)	R & T ($0.07 \le x \le 0.08$), R ($0.08 < x$)	200	317 (x = 0.08)	42.9	[126]
2014	$(1-x)$KNN-xBNKLZ, (x = 0−0.07)	O & R, R & T ($0.03 < x \le 0.05$), R ($0.05 < x \le 0.07$)	300 $\le T_c$	236 (x = 0.04)	38	[127]
2014	0.92KNNLx-0.02BKT- 0.06BZ, (x = 0−0.05)	R ($x < 0.03$), R & T (x = 0.03)	235 $\le T_c$	227 (x = 0.03)	39.3	[128]
2014	$(1-x)$KN$_y$NS$_z$-xBNK$_w$Z, ($0 \le x \le 0.05$, $0.40 \le y \le 0.68$, $0 \le z \le 0.08$, and $0 \le w \le 1$)	R & T	217 $\le T_c \le$ 304	490	–	[129]
2014	$(1-x)$KNNS-x BNKPZ, (x = 0−0.06)	R & T ($0.035 < x \le 0.045$), R ($0.05 \le x \le 0.06$)	200 < T_c	460 (x = 0.04)	46	[130]
2014	$(1-x)$KNN-xBNLZ, (x = 0−0.06)	R & O, O & T (x = 0.04), R ($0.04 < x$)	350	242 (x = 0.04)	33	[131]
2014	(0.99-x)KNN-0.01BNT-xBNKLZ, (x = 0−0.06)	R & T ($0.03 \le x < 0.05$)	338 $\le T_c$	310 (x = 0.035)	45	[132]
2015	0.92(Na$_{0.5}$ K$_{0.5}$)NbO3- (0.08x) (Bi$_{1/2}$ Li$_{1/2}$) TiO$_3$$x$BaZrO$_3$	R & T ($0.05 \le x < 0.06$)	250 $\le T_c$	~ 350 (x = 0.06)	58	[133]

[a] R, O, and T are referred to as rhombohedral, orthorhombic, and tetragonal phase, respectively.

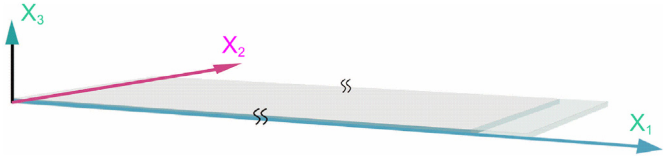

Fig. 1. A schematic diagram of plate type piezoceramics.

As mentioned, the resonance frequencies depend critically on the type of vibration mode and the geometry of piezoelements. However, one thing to be noted is the fact that the resonance/antiresonance frequencies change with the presence of an external load capacitor, meaning that the electromechanical coupling coefficient decreases. When the load capacitor is connected parallel to the piezoelement, the resonance frequency remains the same but the antiresonance frequency shifts down. On the other hand, when the load capacitor is connected serially, only the resonance frequency increases. (See Fig. 3) The changed resonance or antiresonance frequency denoted as f_L is given as

$$f_L = f_s\left[1 + \frac{C_1}{2(C_0 + C_1)}\right]. \tag{11}$$

2.1.2. Mechanical quality factor

Quality factor is generally defined as a parameter that represents a 'resistance' to damping of oscillators or resonators. This means that the higher the quality factor, the more stable the performance of oscillators during operation. In the case of piezoelectric materials as a mechanical vibrator, a special attention is paid to the mechanical quality factor (Q_m), which is defined as

$$Q_\mathrm{m} = \frac{f_s}{\Delta f}, \tag{12}$$

where f_s denotes the resonance frequency of the given vibration mode. Δf is the difference between two frequencies given at the point where the absolute impedance is $\sqrt{2}$ times larger than that at the resonance frequency as schematically illustrated in Fig. 2(a). This means that the mechanical quality factor is directly related to the sharpness of the resonance

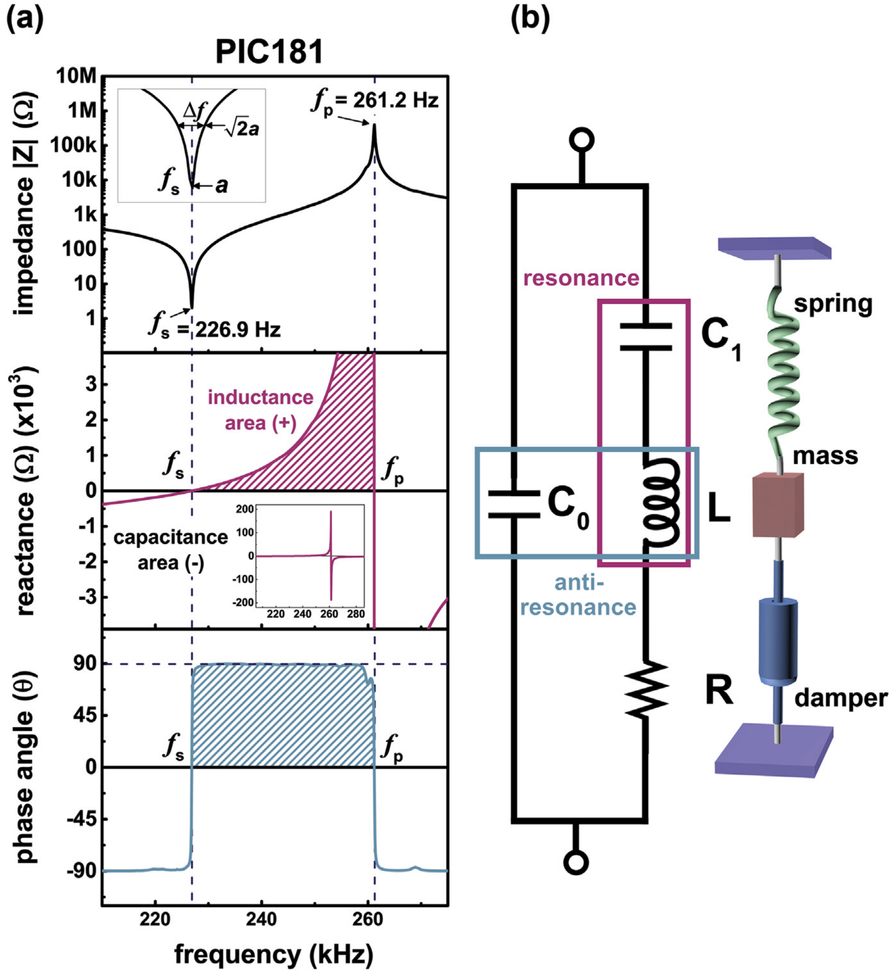

Fig. 2. (a) Impedance, reactance and phase angle change of a commercial hard PZT ceramic (PIC181) around its planar resonance and antiresonance frequency. (b) Equivalent circuit of piezoelectric materials near the resonant frequency. This model consists of a parallel connection of a series *LCR*, denoting mechanical mass, elastic compliance, and damping, and a electrostatic capacitance.

peak. Considering the symmetry of the resonance peak [135], it is easily grasped that the sharper the peak, *i.e.*, the smaller the Δf, the smaller the distance between the resonance and antiresonance peak, *i.e.*, the smaller the electromechanical coupling factor. Given that the heat generation during vibration at the resonance frequency mainly comes from the mechanical loss, *i.e.*, the reciprocal of mechanical quality factor, a high Q_m material is usually preferred for high power applications. However, if Q_m is too high, the frequency characteristic is too sensitive to control. Therefore, Q_m needs adjusting depending on the target applications.

2.2. Doping as an effective processing variable

One of the main features making PZT's so versatile is that the piezoelectric properties can be easily tailored by chemical modifications. To better understand the effect of chemical modifications, it is often useful for one to visualize the perovskite structure beyond the typically-adopted unit cell represented by a single ABO_3 unit. It means that once the perovskite structure is seen at a mesoscopic scale with cations blinded as shown in Fig. 4(a), one can easily see it as a 3-dimensional network composed of corner-shared oxygen octahedra. This specific structure allows individual oxygen ions to easily move through the crystal by switching their position with nearby oxygen vacancies [136,137]. As well, this specific array of oxygen octahedral network provides additional important substitutional sites for cation incorporation, *i.e.*, the center of cubooctahedron, where the coordination number goes 12. In short, the perovskite structure can be understood as a 3-dimensional oxygen octahedral network with two types of cations (A^{2+} & B^{4+}) occupying octahedral and cubooctahedral center as schematically illustrated in Fig. 4(b).

Three types of chemical modifiers are of a general concern, *i.e.*, an acceptor that lacks an electron, a donor that possesses an extra electron, and an isovalent dopant in reference to the prototypical $A^{2+}B^{4+}O_3^{2-}$. An isovalent substitution could lead to changes in the lattice parameters and consequent changes in the Curie temperature, changes in elastic or electrical properties, *etc.* Given that the effect of isovalent substitution depends highly on the nature of individual ions, a general description is practically impossible at the moment yet; thus, we only focus on the effect of heterovalent substitution here, the effect of which shares characteristic features regardless of the kind of ions [32]. When an acceptor substitutes for the *A*-site or *B*-site cations in perovskite structure, *e.g.*, monovalent ions such as Li^{+} replacing divalent Ba^{2+} or divalent ions such as Mg^{2+} or trivalent ions such as Fe^{3+} replacing tetravalent Ti^{4+} in $\mathrm{BaTiO_3}$, oxygen vacancies are created around the acceptor ions to compensate the electron deficiency and are bound to the acceptor ion to form a defect dipole. A similar story goes with the substitution of donor either for divalent *A*-site with the ions of a higher valence such as the trivalent La^{3+} or tetravalent *B*-site with pentavalent ions such as Nb^{5+}. To keep the charge neutrality, cation vacancies are generated and form defect dipoles with the donor ions. The defect dipoles typically generated by acceptor and donor dopings are schematically presented in Fig. 5.

When a defect-generating dopant is introduced to a perovskite lattice, it creates defect dipoles during high temperature heat-treatment, typically during calcination. Once formed, these dipoles are randomly oriented, keeping cubic symmetry statistically in the lattice. When the material cools down to and below the Curie temperature, ferroelectricity sets in, manifested by the appearance of a spontaneous polarization, the direction of which is determined by the crystal symmetry, *i.e.*, //(001), //(111), and //(110) in tetragonal, rhombohedral, and orthorhombic symmetry, respectively. As discussed above, the defect dipoles between acceptor and oxygen vacancy can easily reorient about the oxygen octahedra; thus, they tend to align along the spontaneous polarization direction to reduce the electrostatic energy [138]. The depolarization field imposed by the aligned defect dipoles is commonly called ‘internal bias’ field. The magnitude of internal bias field can be estimated by an offset along the electric field axis in the polarization hysteresis loop measured after electrical poling treatment as exemplarily shown in Fig. 6(a) [139−141]. It is well-known that the presence of internal bias field prevents domain walls from moving easily through domain wall pinning effect. This leads to a great enhancement in the mechanical quality factor, which is a desired property for high power/voltage applications. On the other hand, the presence of internal bias field in unpolarized materials causes the hysteresis loop to be constricted as shown in Fig. 6(b). This constriction is a consequence of the depolarization field that brings the

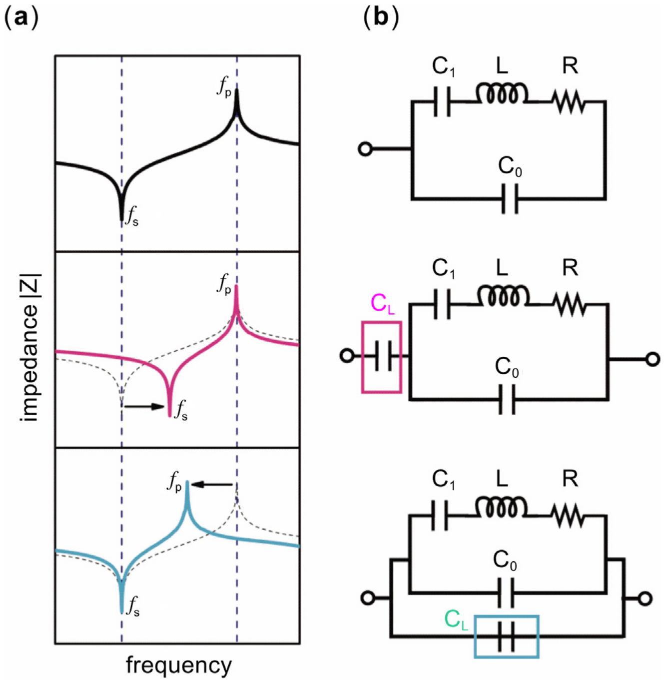

Fig. 3. (a) Impedance changes in the presence of an external load capacitor and (b) its equivalent circuit diagrams.

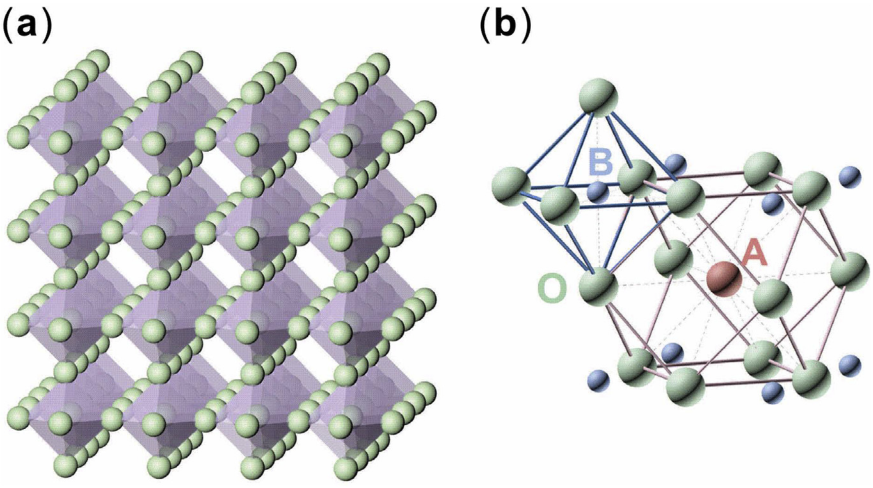

Fig. 4. (a) 3-dimensional network of corner-sharing oxygen octahedra and (b) the octahedral site for the coordination number 6 and the cubooctahedral site for the coordination number 12.

polarization state back to the original state. The constricted hysteresis loop opens with continuous bipolar cycles, which is due to the limited mobility in the reorientation of the defect dipoles. On the contrary, the defect dipoles between donor and cation vacancy stay randomly oriented due to the energy barrier for reorientation originating from the planar oxygen layers. Therefore, this type of defect dipoles makes the materials elastically 'softer', which promotes domain wall motion leading to an enhancement of electromechanical coupling factors as well as piezoelectric coefficients. In this sense, the donor and acceptor dopings are commonly called 'soft' and 'hard' piezoceramics, respectively.

As noted, chemical modification through dopants is one of the most effective and useful methods for tailoring piezoelectric properties. Those effects have been best-realized in PZT-based systems. This is one of the main reasons why PZT is so widely used in industries. This means that facilitated chemical modifiability is a key to a successful development of lead-free piezoceramics as an alternative to PZT-based materials. Presently, not many noticeable successes through this path have been reported on KNN-based materials. Though the effects of donors and acceptors seem consistent in KNN-based systems with those manifested in PZT-based systems [145−148], systematic studies are rare. Instead, most relevant researches still remain processing-related issues [9−11,149].

On the other hand, some relevant studies have been performed on BNT-based systems, which are another important class of lead-free piezoceramic systems. However, the effects seem to lack consistency with those of PZT-based ones possibly due to the inherent relaxor nature of the BNT-based materials. An apparently clear effect of donors was shown to 'strengthen' the relaxor properties, represented by the decrease in ferroelectric-to-relaxor transition temperature (T_{F-R}), while the acceptors do the opposite with T_{F-R} increasing [41,150−154]. Nevertheless, more detailed researches are strongly needed to properly understand the effects.

Isovalent doping effects are that an atom substitutes the atom which has the same atomic valency and a similar ionic radius, for example, Hf^{4+} or Sn^{4+} substitutes $(Zr, Ti)^{4+}$ or Ca^{2+} or Sr^{2+} does Pb^{2+} in PZT [23,32,155−166]. It is known that isovalent dopings affect the dielectric permittivity as well as T_c, though the changes are not so pronounced [167−172]. It is well-known that in BT [173−185], for example, isovalent substitutions shift the polymorphic phase transition (PPT) temperatures [32]. Though the effect of isovalent doping is not so strong, it is still quite a powerful way to tailoring properties of piezoceramics.

2.3. Incipient piezoelectricity

For ferroelectrics to be utilized as piezoelectrics, they must be electrically polarized. The polarization process aligns the polarization direction of the individual domains as near to the electric field direction. Once they are aligned, domain

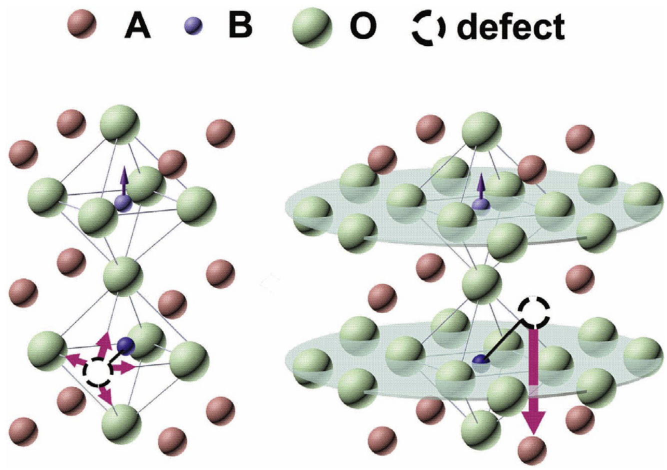

Fig. 5. Typical examples of defect dipoles induced by an acceptor (left) and a donor (right).

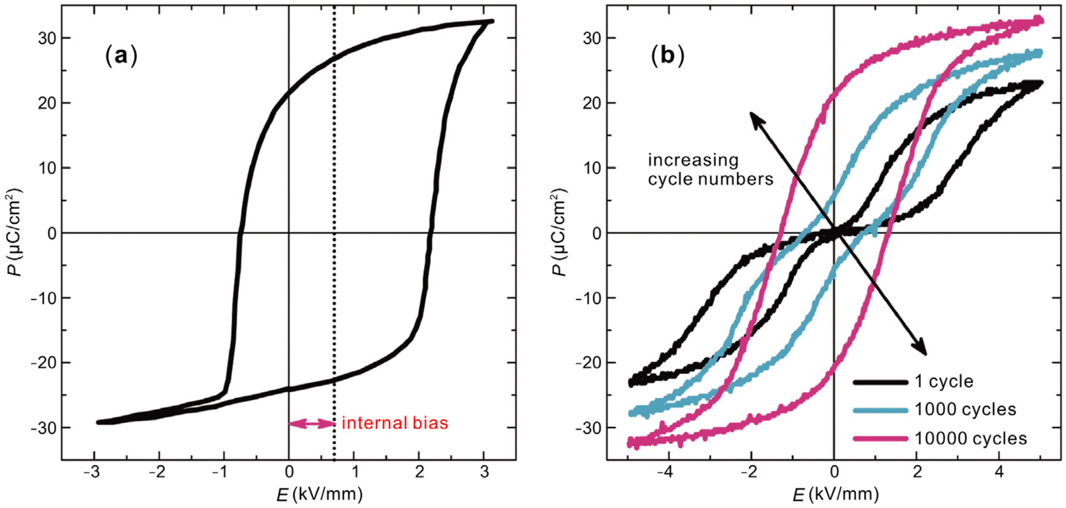

Fig. 6. (a) Polarization hysteresis of an acceptor-doped PZT after high temperature poling process that forcefully aligns defect dipoles along a preferential direction. (b) Evolution of the polarization hysteresis loop of an acceptor-doped PZT as a function of electrical cycling. It is discerned that the initially-existing constriction gradually disappears with cycling [139,142—144].

configuration remain unchanged even after electric field is removed due to the presence of a depolarization field that comes from the charges collected on the electrodes and counterbalances the electrostatic energy due to the alignment of domains. The state at zero electric field after poling is called the remanent state. The existence of this remanent state has an great impact on the electromechanical strains of piezoceramics, especially on the unipolar strains that are important for most actuator applications, because the unipolar strain of a material is equal to the difference between the maximum achievable strain and the remanent strain. In the case of a commercial PZT ceramic, *e.g.*, PIC151, this remanent strain is $\approx 0.2\%$, which is almost as large as its unipolar strain, meaning that the maximum achievable unipolar strain of PZT would be about two times larger than the currently available value without the remanent strain [186].

Since an extremely large strain of $\approx 0.4\%$, which is about two times larger than that of PZT's, was reported on a lead-free 0.92BNT-0.06BT-0.02KNN ceramic in 2007 [90,187,188], a great attention has been paid to the origin of this large strain [189—191]. It was initially proposed that the strain mechanism for this large strain be an antiferroelectric-to-ferroelectric transition after the initial report on a possible existence of antiferroelectric phase in BNT-BT system [38,192,193]. However, the evidence for the antiferroelectricity except for a constriction in the polarization hysteresis was found. Instead, Jones and Thomas [194,195] reported that the originally claimed antiferroelectric phase should be, in fact, a ‘ferrielectric’, which belongs to the ferroelectric category though the spontaneous polarization is considerably small. Though it took quite a while to understand the underlying principle, this puzzle seems to be resolved. A series of reports demonstrated that the origin comes from an electric-field-induced phase transformation from a macroscopically paraelectric to a ferroelectric state, as depicted in Fig. 8(a) [196]. Later, it was proposed that the macroscopically paraelectric state is, in fact, a relaxor state, more precisely an ergodic relaxor (ER) state [197—199]. In fact, it was found that the BNT-BT itself, conventionally considered a normal ferroelectric, is a relaxor, more precisely a nonergodic relaxor (NR), which can be well-grasped from Fig. 8(b).

At this point, it would be useful for us to have a closer look into the relaxor ferroelectrics to better understand the strain mechanism of BNT-BT-KNN system. Fig. 9 is the temperature-dependent dielectric permittivity of a canonical relaxor PLZT ceramic before and after poling. It is seen that two signals are identical above a certain temperature, *e.g.*, T_{VF}, so-called a freezing temperature derived from the Vogel—Fulcher relationship [200,201]. In other words, any change induced by electrical poling treatment above T_{VF} disappears with the removal of electric field, while a permanent change is introduced to the system by electrical poling treatment below T_{VF}. With respect to this difference, the former and the latter are called an ergodic and nonergodic relaxor, respectively. It is noted that an electrical poling treatment brings a long-range

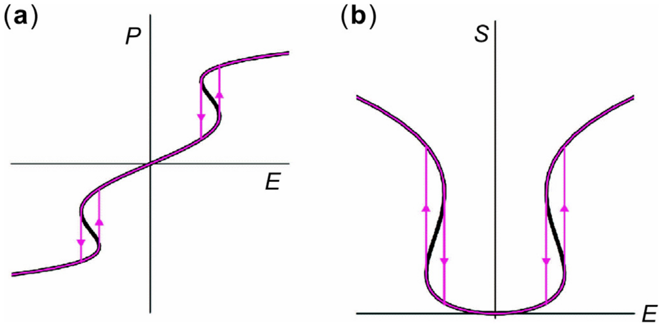

Fig. 7. a) Polarization and (b) strain hysteresis loop at slightly above Curie temperature, predicted by Landau—Ginzburg—Devonshire model.

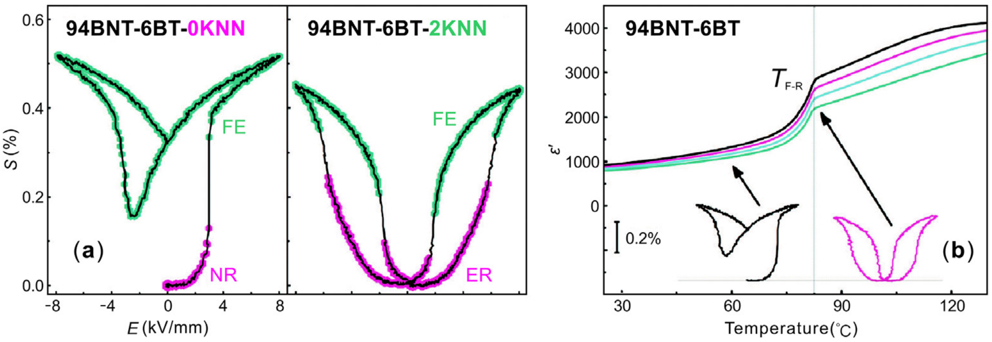

Fig. 8. (a) Electric-field-induced bipolar poling strain of selected compositions in BNT-BT-KNN system, manifesting the appearance of a large strain, and (b) temperature-dependent dielectric permittivity of poled 0.94BNT-0.06BT with three representative strain behaviors below, near, and above the ferroelectric-to-relaxor temperature (T_{F-R}). FE denotes ferroelectric.

ferroelectric order into the system permanently, which is obvious from the disappearance of frequency dispersion in the dielectric permittivity as well as the presence of remanent polarization [202,203]. Here, the macroscopically-induced ferroelectric order vanishes at T_{F-R}, which matches nicely with T_{VF} as well as the depolarization temperature represented by T_d through thermally-stimulated-depolarization current (TSDC) measurement, though T_{F-R} do not have to be identical with the other two temperatures [15].

Ironic as it may sound, this large strain could be understood even without understanding the relaxor-related issues, because it is predictable simply by the Landau−Ginzburg−Devonshire (LGD) phenomenological model. Fig. 7(a) and (b) present the polarization and strain hysteresis loop calculated using the LGD model on BT slightly above T_C. A paraelectric to ferroelectric transformation evidenced by the double hysteresis in the polarization hysteresis loop is clearly discerned, which was experimentally confirmed on a BT single crystal [15]. What is noted is that this electric-field-induced phase transformation is reversible, because the stable phase at zero-field state is a paraelectric. The LGD model explains that the large strain originates from a reversible phase transformation from a paraelectric to a ferroelectric state without any remanent state that is inherent to normal ferroelectrics. It follows that this type of a large strain can be realized in any material system that undergoes a reversible phase transformation from a macroscopically paraelectric to a ferroelectric such as paraelectric slightly above T_C, ergodic relaxor, antiferroelectric, ‘hard’-type piezoceramics. Given that this large strain appears mainly during the phase transformation to a ‘piezoelectric’ state, we proposed that these materials be called the ‘incipient’ piezoelectrics [15], the underlying mechanism of which can be related to the recently proposed polarization extension concept [60].

The incipient piezoelectric effect, in principle, guarantees extraordinarily large strain through a reversible phase transition from a macroscopically paraelectric to a ferroelectric (or piezoelectric), because each unipolar cycle is a repeat of poling cycle [196]. There are some drawbacks in the large strain from the practical point of view, depending on the type of incipient piezoelectrics. For example, in the case of a normal ferroelectric such as BT above the Curie temperature, this large strain can only be induced in a narrow temperature range, because the magnitude of electric field required for inducing the phase transformation increases sharply with temperature [55]. As well, the incipient piezoelectric strain induced in antiferroelectrics is rather vulnerable to continuous cycling, because an antiferroelectric-to-ferroelectric phase transition accompanies a large volume change [204]. In the case of relaxor ferroelectrics, both temperature stability [188,196,205,206] and cycling stability [207−209] are acceptable, but application field is limited to on/off-type actuators due to their rather large hysteresis.

We may say that the discovery of BNT-BT-KNN system is significant in that it introduced a new way of enhancing the strain properties of lead-free piezoceramics. However, this does not mean that its large strain can be utilized in real-world applications. Two challenges are evident; one is the extremely large electric field required for activating this strain and the other the relatively large hysteresis. Given that the large hysteresis originates from the incipient piezoelectricity itself, most studies so far have focused on reducing the

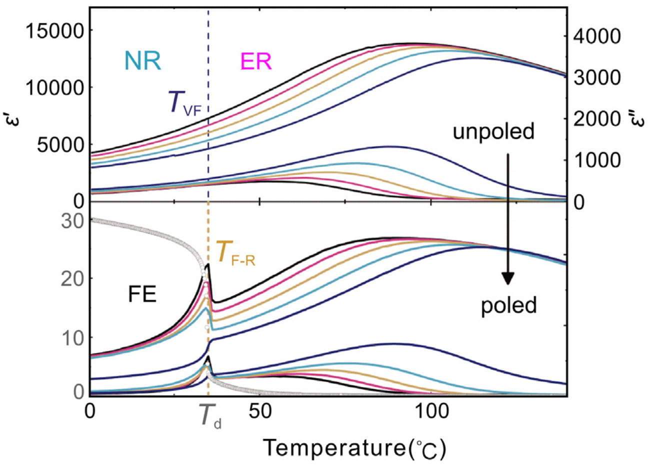

Fig. 9. Temperature-dependent dielectric permittivity of an 8/65/35 PLZT ceramic before (top) and after (bottom) electrical poling, which presents the unique features of relaxor ferroelectrics.

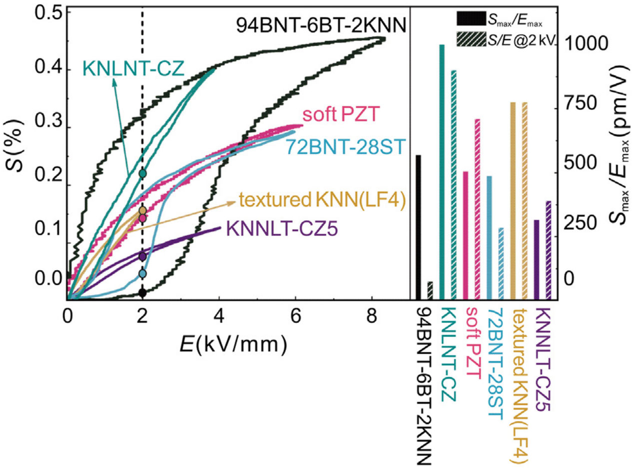

Fig. 10. State of the art in the accomplished strain behaviors via incipient piezoelectricity in comparison with that of commercial soft PZT (PIC151, PI Ceramics, Germany) and textured KNN [6], KNNLT-CZ5 [113], BNT-28ST [210].

required electric field [15,191,211–213]. Naturally, a number of new compositions have been reported [214–224] resulting in the discovery of 0.72BNT-0.28ST, the strain property of which competes that of PZT even at 3 kV/mm as shown in Fig. 10 [210,225]. Apart from the compositional studies, efforts in enhancing strain properties based on processing have been made. It was demonstrated that once one can induce a core–shell structure where the core is ferroelectrically active and the shell is paraelectric, not only the required field for activating strains but also the hysteresis in the strain decrease notably [226]. It was further shown that the property enhancement using a core–shell structure can be realized simply by 0–3 type ceramic–ceramic composites, which consist of a macroscopically paraelectric composition as a matrix (3) embedded with a certain amount of a ferroelectrically-active composition (0) [211,227]. The state of the art in tailored strain properties is summarized in Fig. 10.

3. New applications and a perspective

All the piezoelectric materials are, in a broad sense, a transducer that refers to materials converting one form of energy into another. This transducer in a broad sense can be classified into four categories, *i.e.*, actuators, sensors, transducer (in a narrow sense), and generators from the application point of view. These four categories again can be specified as shown in Fig. 11. Global market size for these piezoelectric devices is expected to grow up to 38.4 billion US dollars by 2017, with a compound annual growth rate of 13.2%. This diagram of the global market for piezoelectric devices lists an individual market share of eleven broad types of devices such as actuators, ultrasonic motors, Langevin actuators, piezoelectric transformers, resonators, transducers, piezoelectric generators including energy harvesters, sonars for military and civilian use, piezoelectric sensors and accelerators, acoustic devices, *etc.* The main application fields of these devices are represented by nine broad application areas such as biomedical applications, information technology/robotics, precision machines, ecological/energy harvesting, nondestructive testing transducers and measurement, piezoelectric sensors, acoustic devices and resonators, sonars for military and civilian use and an additional group that includes ultrasonic welding, ultrasonic cutting, gas ignition, and other applications.

In spite of the variety of applications and their growing market size, search for new applications is always on-going in the related industries. This is partially because the advancement in alternative technologies is so fast that the existing market is subject to be taken over by them at any time. Therefore, this section intends to prospect potential applications where the use of lead-free piezoceramics can be considered after overviewing selected new applications recently introduced both in lead-based and lead-free piezoceramics.

3.1. Lead-based piezoelectric components

This section snapshots lead-based piezoelectric devices, newly introduced to the market as an emerging technology. Most applications to be introduced hereafter adopt multilayer actuators, where the low-temperature co-firing for cheaper electrodes always remains a great challenge. Given that the piezoelectric materials, in definition, utilize the electromechanical coupling, the mechanical stability is still another challenge to overcome. Nevertheless, we hope that this brief overview enables one to have at least a rough idea where the industry heads for and what are the usual considerations for the selected new applications.

3.1.1. Piezo actuator for bone conduction by Kyocera

Our hearing is based on sensing sound waves that are altered in air pressure. These sound waves are perceived through two pathways. One is through air conduction, meaning that the sound waves directly move through the ear canal, vibrating the eardrum. This vibration is transmitted to the air-filled ossicles and then to the fluid-filled cochlea through an impedance matching between air and water. The other is through bone conduction that reinforces the air conduction. Although the exact mechanism for the bone conduction is still not fully clarified, it is obvious that the hearing through the bone conduction takes place directly at the basilar membrane inside the cochlea [228]. The reason why the recorded voices of ours sound different to us is due to the absence of bone conduction in them. Although the air conduction is the major source for hearing, a catch is that it is vulnerable to the ambient noise. In contrast, the bone conduction is free of such problems.

In 2012, Kyocera Corporation released an innovative audio device, called *Smart Sonic Sound*™ that is featured by the ‘speaker-less’ speaker function. The working principle is to let one hear sounds based on the bone conduction mechanism

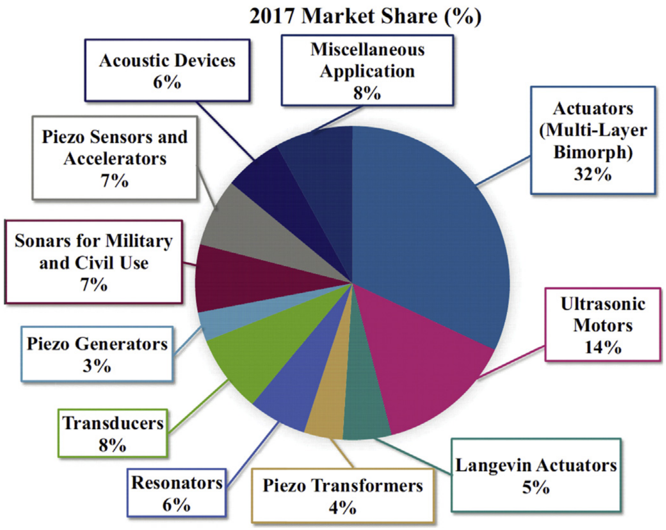

Fig. 11. Estimation of the market share of piezoelectric devices in 2017. Source: iRAP, Inc. (2013).

through the waves generated on the whole display panel by a vibrating film-type piezoelement, as schematically shown in Fig. 12. To hear the sound from the smartphone, all one has to do is to press the display panel against any part of the head even against the earmuffs. The innovation comes from the fact that this technology allows one to hear the desired sounds even in the midst of noisy environments such as in a crowded bar or in the places where noise should not be made such as in a library. Furthermore, this technology is highly promising for hearing aid applications.

The piezoelement used for the *Smart Sonic Sound*™ is featured by ultrathin ($\leq$1.5 mm) and light weight ($\leq$23 g) as well as low directivity and high responsivity that create a high quality sounds. This device uses a 'monomorph'-type piezoelement that vibrates alone without metal plates. Since the operation is through a 31-mode, d_{31} becomes the figure of merit. Given that the piezoelectric coefficient matters, this piezoelement can also be utilized in a wide range of applications such as actuators for diesel engine vehicles, inkjet printer head with its fast response time and high reliability.

3.1.2. Piezo actuator by SEMCO

In game consoles and smartphones where a vibrational notice function is no longer an option, a vibrating motor is used to generate such signal, which is commonly called a haptic (a feeling based on the sense of touch) function. So far, linear actuators have been largely employed due to their relatively cheap price with a moderate functionality. Recently, however, a great attention has been paid to piezoelectric actuators due to their superior functionality. Piezoelectric actuators are featured by a rapid response time, a wide frequency bandwidth, variable frequencies, and a high-definition signal, which provide delicate and diverse haptic functions (see, for example, Fig. 13). Samsung Electro-Mechanics (SEMCO) announced their successful mass production on a bar-type piezo haptic actuator utilizing a radial vibration mode. This vibrating piezoelement is glued on a metal plate with which vibrations create bending motions, utilizing a 31-mode. A general information of the SEMCO piezo actuator is summarized in Table 2.

The key to achieving excellent haptic performance is to secure as high acceleration as possible. The unit for the acceleration is expressed in terms of G, which corresponds to the acceleration from gravity. The reason why G is used instead of a force (N) or a displacement (mm) is that the piezoelement is supposed to vibrate a certain mass attached to it. It means that even the same piezoelement results in a different performance depending on the type of mass attached to it, since we need to take the whole system, *i.e.*, piezoelement as well as the attached mass, into consideration for a proper evaluation. The acceleration realized in the device is directly related to the vibrating amplitude of the piezoelements. Therefore, the piezoelements for the haptic applications are made through multilayer technology to maximize the displacement as large as possible. However, the multilayer technology inevitably increases the capacitance of the piezoelement, the upper limit of which is restricted by the circuit. Therefore, the desired

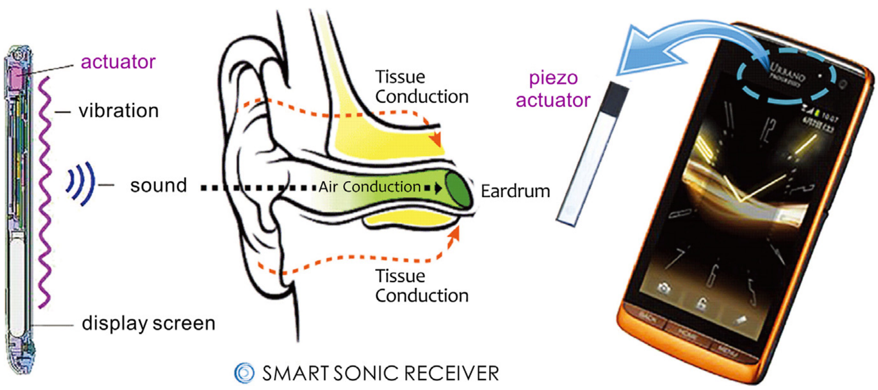

Fig. 12. A smartphone featured by a 'speaker-less' function based on a bone conduction mechanism. The vibration for the bone conduction is realized by a piezoelectric element. Retrieved from http://www.kyoceramobile.com/smart-sonic-receiver/.

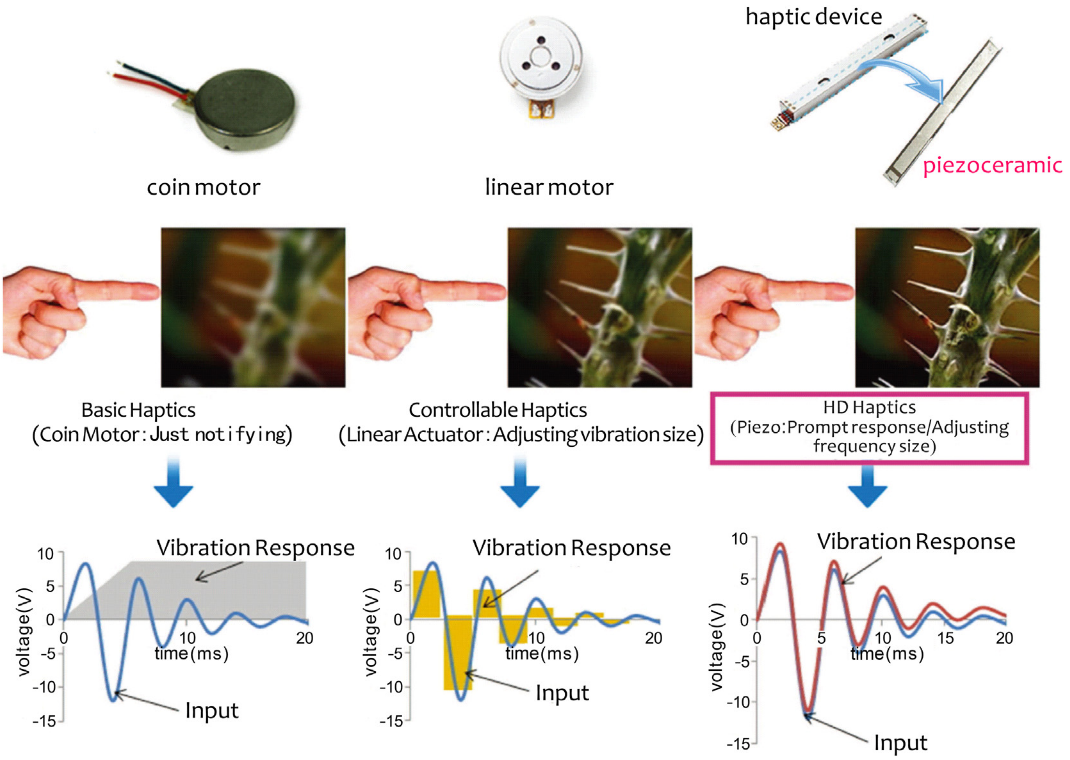

Fig. 13. A comparison of haptic functions realized by different technologies, clarifying the superiority of piezoelectric technology for this purpose. Piezoelectric haptic actuator with the embedded piezoelectric element (Samsung Electro-Mechanics Co. Ltd. The advantage of piezoelement for haptic functions is clearly seen by the comparison with other elements. Retrieved from http://www.samsungsem.com/global/product/module/vibration/piezo-actuator/index.jsp.

properties of piezoelements for haptic applications are as high d_{31} and small capacitance as possible.

3.1.3. Vibrating piezo-speaker by Pantech

Speaker is an electronic transducer that converts an electrical signal to a sound wave. Most commonly used speakers are based on a magnetic system, which is heavy and large in size. As noted, one of the most pronounced advantages that piezoelectric-based devices have is its dimensional advantages for small-scale applications. The entire module can be as thin as ~2 mm or less, which is by far smaller than its magnetic counterpart. There have been a number of attempts to realize piezoelectric speakers for various applications such as in tweeter, computers, watches, *etc.* One of the best application fields of the piezoelectric speaker is the sonar, which has advantages over magnetic-based ones due to its simplicity and a better resistance to seawater. In 2013, Kyocera successfully incorporated their *Smart Sonic Sound*™ into thin television with high-quality sounds in a 180-degree audibility.

Pantech Corp. recently announced in a press release that they have developed a vibrating piezoelectric speaker in cooperation with Innochips technology Co., Ltd., which enables smartphone users to enjoy an extraordinary experience. This piezo-speaker installed as an add-on to a smartphone as presented in Fig. 14 creates a sound loud enough to be used outdoor activities, when it is place on any hollow object. It is known that the operation principle of the piezoceramic in the device is almost identical with that of *Smart Sonic Sound*™, and the material characteristics is similar to the one used for haptic applications.

3.1.4. Micro blowers

A trend in today's industries demands devices that require smaller dimensions, light weight, low power consumptions, and reduced heat generation. This challenging trend consequently forces developers to come up with taxing technological breakthroughs. One of such examples can be found in a recently introduced viscosity sensor [230]. Another example is the cooling technology for electronic devices. The importance of this field is best-visualized by the number of proposed alternative technology to the conventional ones such as gas-based and fan-based ones [231]. Currently, micro blowers based on piezoelectricity seems the nearest to practical applications with their extreme compactness, practically zero

Table 2
Specifications of the SEMCO actuator for mobile applications.

Properties	Unit	Bar piezo
Size	mm	35 × 110 × 3.8
Rated voltage	V_{rms}	AC 42 (120 V_{pp})
Frequency	Hz	230
Capacitance	nF	30 nF ± 30%
Acceleration @100 g phone JIG.	G_{rms}	Min. 1.25

noise, and low power consumption. The piezo-micro blowers as presented in Fig. 15 function as an air pump discharging high pressure air through ultrasonic vibration of piezoceramics. The device is typically driven at a resonance mode with the piezoelement being attached to a metallic diaphragm that bends due to vibrating piezoelement in a 31-mode. Though an immediate application field could be alternative small-scale cooling device applications, the application field can be extended to an air blower for fuel cells, particulate diffusers using a high speed airflow, aromatic atomizers or air refresher for household fragrance products, *etc.*

3.2. Lead-free piezoelectric components

While the efforts have been made on to come up with new creative applications using the conventional lead-based piezoceramics as briefly introduced in the previous section, attempts to replace the lead-based piezoceramics with lead-free ones have significantly increased on the industry side over the last decade. At the moment, the use of lead-free piezoceramics is strictly limited to applying for already existing devices, we hope that a completely new type of applications made possible only with lead-free piezoceramics would show up in a near future. This section presents some of the exemplary products which have quite successfully replaced the conventional lead-based piezoceramics with lead-free ones mainly for transducer applications.

In 2014, PI Ceramic GmbH announced that they successfully mass-produced a lead-free piezoceramic, called PIC700. The aimed major application field was industrial ultrasonic transducers operating in the MHz frequency range including sonar and hydrophonic applications as seen in Fig. 16(a) [232,235]. The most notable achievement is the large quantity of ~50 kg they can manufacture through a single processing cycle. The PIC700 is featured by a strong anisotropic behavior in its electromechanical coupling factors, offering suitable conditions for sensor and transducer applications.

HanaUtech Co., Ltd. applied a KNN-based lead-free piezoceramic to an auto-focusing module for an interchangeable-lens camera, as presented in Fig. 16 [233]. Although functionality turned out to be inferior to that using a PZT-based piezoceramic, they demonstrated that it is very near to commercialization with a moderate performance.

Slightly before PIC700 was presented by PI Ceramic GmbH, Honda Electronics Co., Ltd. introduced a BNT-based lead-free piezoceramic transducer for ultrasonic cleaner applications, as depicted in Fig. 16(c) [234]. Although most functional properties including two most important ones such as the mechanical quality factor and the electromechanical coupling factor measured according to the standard measurement techniques are inferior to those of a hard PZT except for mechanical properties, the stability of mechanical quality factor against vibration velocity as well as input power turns out to be by far better, making it highly suitable for commercial uses. Transducers for ultrasonic cleaning are used not only for cleaning but also for stirring, defoaming, and many other applications. With its load stability, this type of transducer is best-suited for gaining high output power. However, the exact mechanism why this load stability of mechanical quality factor arises is left for the academia to come up with a reasonable explanation.

On the other hand, NGK Co., Ltd. patented an alkali niobate/tantalate type perovskite oxide to be used in a non-resonant type knock sensor, as presented in Fig. 16(d) [236]. Piezoelectric knock sensor detects the vibration caused by engine knocking, enabling the ignition timing control that contributes to improved engine performance and fuel economy. The developed item is featured by a flat output over the knock frequency band of 5–15 kHz allowing a flexibility for the use in a variety of engines. For this use, they developed piezoceramics that have a high output and low-temperature dependence.

Fig. 14. External look of the smartphone with an embedded piezo-speaker (left) and the piezoelectric module inside (right) [229].

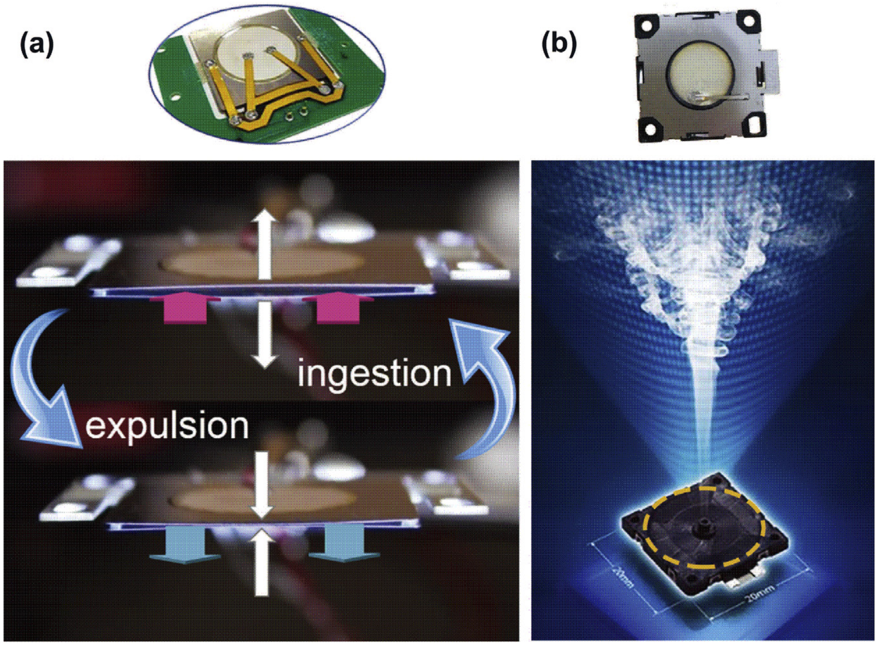

Fig. 15. Piezoelectric-based micro blower introduced by (a) General Electric Co. (Retrieved from http://www.geglobalresearch.com/innovation/ges-dual-piezoelectric-cooling-jets-dcj-cool-quiet) and (b) by Murata Co., Ltd. (Retrieved from http://www.murata.com/en-us/products/mechatronics/fluid/feature).

3.3. General applications

3.3.1. Figure of merit for general applications

Typical parameters such as piezoelectric coefficients and electromechanical coupling factors regardless of the types of applications had been considered for developing piezoceramics until Uchino et al. in 2003 [135] came up with five parameters as figures of merit for specific applications, namely, piezoelectric charge coefficient (d), piezoelectric voltage coefficient (g), electromechanical coupling factor (k^2), mechanical quality factor (Q_m), and acoustic impedance (Z) depending on the type of applications. More precisely, what was proposed was that one should consider such parameters as electrical requirements, processing conditions, operation environments during the design and the selection of materials. For most cases, this consideration works fine, but more functional and detailed classification to be used as the figure of merit is demanded since the application field of the materials is broadened and sophisticated.

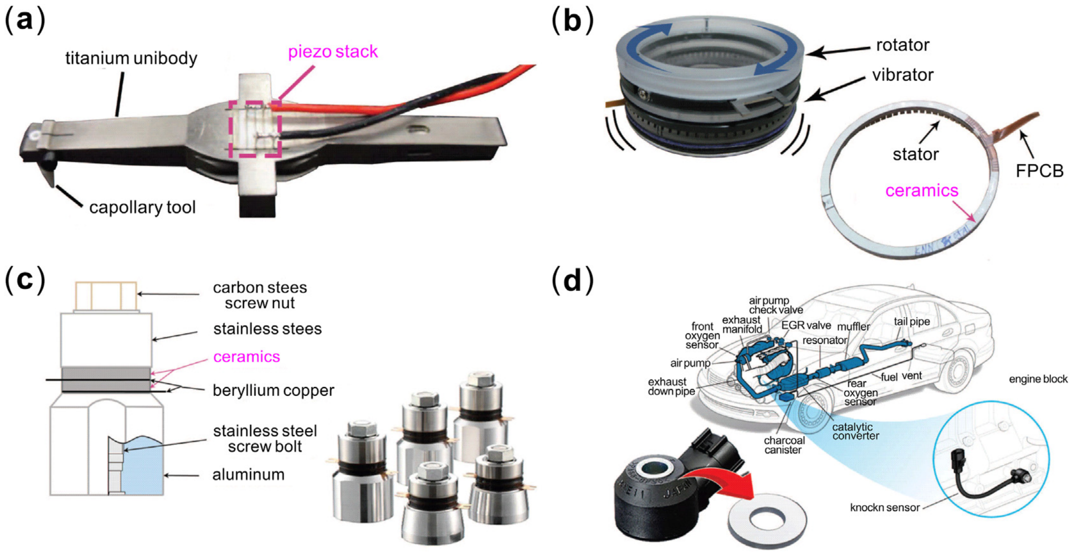

Fig. 16. Piezoelectric devices realized by lead-free piezoceramics. (a) Piezoelectric transducer using a lead-free BNT piezoceramic [232], (b) a ring-type rotary ultrasonic motor using KNN-based ceramics by HanaUtech, Co., Ltd. [233], (c) the first commercial BNT-based piezoelectric transducer for ultrasonic cleaning application [234], and (d) a knock sensor for automobile engine monitoring by NGK, Co., Ltd. (Retrieved from http://www.ngkntk.co.jp/english/csr/pdf/csr2013we.pdf).

Rödel et al. [8] proposed the required properties both of lead-containing and of lead-free piezoceramics for specific applications. To come up with the figures of merit for each application, they consider the maximum operational temperature as the most important parameter, because it is a fundamental requirement imposed by the application itself. Once the material meets the temperature requirement, it is further classified into two categories depending on the mode of operation, resonance or off-resonance driving. In the resonance mode, the mechanical quality factor Q_m or the product of the Q_m and the electromechanical coupling factor k^2 matters. The Q_m as a figure of merit is justified by the fact that low Q_m results in a heat generation during operation, leading to a thermal degradation of the material. During the vibration at the resonance frequency, the impedance hits its minimum value, where the stored energy becomes the maximum, *i.e.*, the maximum k^2 at the resonance. As well, k^2 is directly related to the frequency bandwidth for the operation. Therefore, resonance-mode applications except for high-power applications require as high k^2 as possible. In the meantime, the magnitude of strain in the resonance mode is proportional to Q_m. The reason why k^2 and Q_m are simultaneously evaluated is partly because these two parameters have a trade-off relation and partly because either k^2 or Q_m should be weighted more depending on the applications though both are still important, *e.g.*, k^2 and Q_m are more important in transducers and in resonators, respectively.

On the other hand, the figure of merit for the non-resonance applications is usually given either by $d \cdot g$ or by S_{max}/E_{max}. In the off-resonance mode, k^2 is not usually considered because it is already too small due to high impedance. Note that k^2 is determined by the width of 'inductance' region, which requires a successive serial and parallel resonance. It follows that Q_m that is proportional to the strain level 'at the resonance mode' [135] is no longer considered in the off-resonance mode, either. Instead, the piezoelectric charge coefficient such as d_{31} becomes important, since the strain level is directly proportional to it. For example, in the case of high-stroke actuators, *esp.*, on-off type actuators, such as for fuel injectors, air valves for car seat adjustment, *etc.*, a highest possible S_{max}/E_{max} is desired. In this case, only the magnitude of displacement matters, meaning that recently reported incipient piezoceramics with large strains can be safely used in spite of the hysteresis in the strain behavior [90].

Other than the high-stroke applications, $d \cdot g$ is normally considered the figure of merit. As in the case of the figure of merit for resonance mode, *i.e.*, $k^2 \cdot Q_m$, d and g that also has a trade-off relation is used as the figure of merit to prevent any numerical misleading, meaning that at an extreme end, g could be greatly enhanced only by reducing dielectric permittivity though d value is impractically small.

These classifications of the figure of merit are a basic consideration for the materials and device developers. Although a certain material qualifies these requirements, there are still further considerations, which is not trivial for commercialization. The following section briefly discusses these additional requirements.

3.4. Additional but non-trivial considerations

3.4.1. Stationary installations

The usual environment for the industrial installations under operation retains an ambient condition, meaning that not much change happens in the level of humidity and temperature. It is of course that highly delicate processing environments such as during semiconductor-related processing maintain an extremely constant condition. In this case, the properties at an ambient environment are more important than their temperature stability. It means that as long as the desired properties of materials such as strain properties, blocking forces, cycling stability, and/or mechanical durability are good enough near the target temperatures, the materials are safely used, though the range of temperature for stable operation is small. Such applications includes the piezoelements for atomic force microscopies, for thread-guide machines, for probe stations, for mask aligners, for pattern generators, for autofocusing module of optical devices, for inkjet printer heads, for superfine laser cutters, *etc.* For these applications, the lead-free piezoceramics such as (Ba, Ca) (Ti, Zr)O_3 and BNT-based incipient piezoceramics are expected to be rather easily manipulated.

3.4.2. Multilayer actuators

One of the most typical types of piezoelements is prepared through a multilayer technology. This technique has been applied to various materials including lead-free piezoceramics [237–239]. When piezoelements are embedded into devices, various electrical properties such as operational voltage, power consumption, and capacitance are enforced to be met for an electrical matching with the connected circuits. Among the requirements, the capacitance often causes a challenge to the material design, because the capacitance of even exactly the same material differs depending on how it is prepared. For example, when a material is prepared as a multilayer piezoceramic, the capacitance changes significantly as a functions of the thickness of each layer and the number of layers. The enforced requirements are the major reasons why the number of layers or the input voltage cannot be increased as desired to enhance the performance of piezoelement. As well, as the capacitance increases, the response time due to capacitor charging and the power factor, represented by cosθ due to the presence of phase angle difference between L and C component, decrease sharply. This eventually leads to the increase in the power consumption and the overall decrease in the performance. In this case, one big advantage of using piezoelement, namely, a higher energy efficiency over competitive technologies, is lost. It follows that when a material composition is designed and developed for a certain application as a multilayer type, the figure of merit needs to be adjusted depending on the device structure and requirements. A general suggestion is that the permittivity is better to be as low as possible even at the expense of other functional properties. For this reason, BNT-based materials seem to be promising.

3.4.3. Surface Mount Devices

Many electrical modules embedded with piezoelements are manufactured by so-called surface mount technology (SMT), where the electronic components are mounted or placed directly onto the surface of printed circuit boards (PCBs) with a soldering paste or a cream solder. For the SMT process to be finalized, the entire PCBs should undergo so-called a ‘reflow’ process, which is to melt the soldering paste to fix each component on the PCBs. This process usually takes place in the temperature range of 250–280 °C for tens of seconds to minutes. Therefore, once piezoelements are supposed to be a part of surface mount device (SMD), the maximum temperature where the poling state survives is the most important factor, regardless of their functional properties. Even though SMT is not utilized, many applications are to be exposed to a somewhat unexpected processing route such as gluing or epoxy bonding that require 150–200 °C for a hardening process. In short, even material developers need to have an idea of the entire processing routes when a target application is in mind.

3.4.4. Geometrical considerations

When one considers to substitute lead-free piezoelements for lead-based ones in the existing products, he or she often faces a trouble with a poorer performance. This is not only because the basic properties of lead-free piezoceramics are inferior to those of lead-based ones, but also because the shape and dimension where the piezoelement is supposed to be embedded are best-tuned for the conventional lead-based ones. However, an important aspect that is often neglected is that the inferiority of functional properties can be covered to a degree by modifying related circuit designs, and that the space limitation can also be resolved by changing vibration modes or the way the piezoelement is embedded. Ideally, the aforementioned problems would disappear if the device design took the shape, location, and connection issues of piezoelement firstly into account. This is one of the reasons why the establishment of an intimate collaborational network between academia and industry is important for synergic advancement of lead-free research. For example, the use of lead-free piezoelement as a knock sensor for automobile engines suffers from a shortage in the output power. However, this problem can be rather easily compensated by a modified circuit design and there is a room for overcoming the dimensional restriction in this specific case, which allows the use of KNN-based lead-free piezoceramics. Another example can be found in the use of lead-free incipient piezoceramics for piezo haptic devices, where the limited output power can be easily compensated by signal amplifying driver IC. Furthermore, the comparative superiority in the mechanical durability to soft PZT provides a further room for tuning the functional properties by changing vibration modes or clamping conditions.

4. Conclusions

Facing the situation where research on lead-free piezoceramics is culminated, a goal was set to the restoration of the community activities regarding lead-free piezoelectric research. Research topics inherent to academia were suggested based on a review over the history of the evolution of piezoelectric community. Three major fields requiring further researches were identified: a deeper understanding of the morphotropic phase boundary mechanism, the effect of chemical dopants, and incipient piezoelectricity. As an out-of-box thought, the establishment of a closer collaborational network between academia and industry was considered to be another route to achieving the goal. To this end, the issues that are often neglected by the academic community have been overviewed, such as the meaning of commonly referred functional properties from the practical point of view and a revisit to understanding the figure of merit for applications with which one can use for designing their application-oriented research. It was proposed that the key to achieving our goal, the restoration of active research on the development of lead-free piezoceramics, is how well we can establish better communication channels with industry partners. We hope that this brief review would make at least a small contribution to building a synergic bridge between academia and industry.

Acknowledgments

This work was supported by the National Research Foundation of Korea (NRF) grant funded by the Korea government (MISP) (No. 2014R1A2A1A11053597). JSS acknowledges the financial support from the 2014 Research Fund (1.140037.01) of UNIST (Ulsan National Institute of Science and Technology). CWA is thankful for the financial support from the Basic Science Research Program through the National Research Foundation of Korea (NRF) funded by the Ministry of Education (2015R1D1A3A01019470).

References

[1] Commission Regulation (EU) 2015/628 of 22 April 2015 amending Annex XVII to Regulation (EC) No 1907/2006 of the European Parliament and of the Council on the Registration. Evaluation, authorisation and restriction of chemicals (REACH) as regards Lead and its compounds. 2015.
[2] Directive 2012/19/EU of the European Parloament and of The Council of 4 July 2012 on Waste Electrical and Electronic Equipment (WEEE). 2012.
[3] EU-Directive 2002/95/EC. Restriction of the use of certain hazardous substances in electrical and electronic equipment (RoHS). 2003.
[4] EU-Directive 2002/96/EC. Waste electrical and electronic equipment (WEEE). 2003.
[5] Regulations: Commission Regulation (EU) No 582/2011. 2011.
[6] Saito Y, Takao H, Tani T, Nonoyama T, Takatori K, Homma T, et al. Lead-Free piezoceramics. Nature 2004;432(7013):84–7.
[7] Cross LE. Materials science: lead-free at last. Nature 2004;432(7013):24–5.
[8] Rödel J, Webber KG, Dittmer R, Jo W, Kimura M, Damjanovic D. Transferring lead-free piezoelectric ceramics into application. J Eur Ceram Soc 2015;35(6):1659–81.
[9] Takenaka T, Nagata H. Current status and prospects of lead-free piezoelectric ceramics. J Eur Ceram Soc 2005;25(12):2693–700.
[10] Shrout TR, Zhang SJ. Lead-Free piezoelectric ceramics: alternatives for PZT? J Electroceram 2007;19(1):113–26.
[11] Panda PK. Review: environmental friendly lead-free piezoelectric materials. J Mater Sci 2009;44(19):5049–62.

[12] Damjanovic D, Klein N, Li J, Porokhonskyy V. What can Be expected from lead-free piezoelectric materials? Funct Mater Lett 2010;3(1):5−13.

[13] Aksel E, Jones JL. Advances in lead-free piezoelectric materials for sensors and actuators. Sensors 2010;10(3):1935−54.

[14] Lu Y-Q, Li Y-X. A review on lead-free piezoelectric ceramics studies in China. J Adv Dielectr 2011;1(03):269−88.

[15] Jo W, Dittmer R, Acosta M, Zang J, Groh C, Sapper E, et al. Giant electric-field-induced strains in lead-free ceramics for actuator applications − status and perspective. J Electroceram 2012;29(1):71−93.

[16] Shvartsman VV, Lupascu DC. Lead-Free relaxor ferroelectrics. J Am Ceram Soc 2012;95(1):1−26.

[17] Priya S, Nahm S. Lead-free piezoelectrics. Springer; 2012.

[18] Li J-F, Wang K, Zhu F-Y, Cheng L-Q, Yao F-Z. $(K,Na)NbO_3$-based lead-free piezoceramics: fundamental aspects, processing technologies, and remaining challenges. J Am Ceram Soc 2013;96(12):3677−96.

[19] Coondoo I, Panwar N, Kholkin A. Lead-Free piezoelectrics: current status and perspectives. J Adv Dielectr 2013;3(02):1330002.

[20] Glaum J, Hoffman M, Green DJ. Electric fatigue of lead-free piezoelectric materials. J Am Ceram Soc 2014;97(3):665−80.

[21] Wu J, Xiao D, Zhu J. Potassium-sodium niobate lead-free piezoelectric materials: past, present, and future of phase boundaries. Chem Rev 2015;115(7):2559−95.

[22] Thurnauer H, Deaderick J. Insulating material. Oct 21 1947.

[23] Shirane G, Suzuki K. Crystal structure of $Pb(Zr\text{-}Ti)O_3$. J Phys Soc Jpn 1952;7(3):333.

[24] Jaffe B, Roth RS, Marzullo S. Piezoelectric properties of lead zirconate-lead titanate solid-solution ceramics. J Appl Phys 1954;25(6): 809−10.

[25] Cao W, Cross LE. Theoretical model for the morphotropic phase boundary in lead zirconate-lead titanate solid solution. Phys Rev B 1993;47(9):4825−30.

[26] Amin A, Newnham RE, Cross LE. Effect of elastic boundary conditions on morphotropic $Pb(Zr,Ti)O_3$ piezoelectrics. Phys Rev B 1986;34(3):1595−8.

[27] Ahart M, Somayazulu M, Cohen RE, Ganesh P, Dera P, Mao H-K, et al. Origin of morphotropic phase boundaries in ferroelectrics. Nature 2008;451(7178):545−8.

[28] Cross LE. Relaxor ferroelectrics. Ferroelectrics 1987;76(1):241−67.

[29] Moulson AJ, Herbert JM. Electroceramics: materials, properties, applications. John Wiley & Sons; 2003.

[30] Park S-E, Shrout TR. Ultrahigh strain and piezoelectric behavior in relaxor based ferroelectric single crystals. J Appl Phys 1997;82(4): 1804.

[31] Ge W, Luo C, Zhang Q, Devreugd CP, Ren Y, Li J, et al. Ultrahigh electromechanical response in $(1\text{-}x)(Na_{0.5}\ Bi_{0.5})TiO_3\text{-}xBaTiO_3$ single-crystals via polarization extension. J Appl Phys 2012;111(9): 093508.

[32] Jaffe B, Cook WR, Jaffe H. Piezoelectric ceramics. London: Academic Press; 1971.

[33] Guo Y, Kakimoto K-I, Ohsato H. Phase transitional behavior and piezoelectric properties of $(Na_{0.5}\ K_{0.5})NbO_3\text{-}LiNbO_3$ ceramics. Appl Phys Lett 2004;85(18):4121.

[34] Zhang S, Xia R, Shrout TR, Zang G, Wang J. Piezoelectric properties in perovskite $0.948(K_{0.5}\ Na_{0.5})NbO_3\text{-}0.052LiSbO_3$ lead-free ceramics. J Appl Phys 2006;100(10):104108.

[35] Wang R, Bando H, Itoh M. Universality in phase diagram of $(K,Na)NbO_3\text{-}SrTiO_3$ solid solutions. Appl Phys Lett 2009;95(9):092905.

[36] Takenaka T, Nagata H, Hiruma Y. Current developments and prospective of lead-free piezoelectric ceramics. Jpn J Appl Phys 2008;47(5):3787−801.

[37] Atsushi S, Tatsuya C, Youichi M, Etsuo O. Dielectric and piezoelectric properties of $(Bi_{0.5}\ Na_{0.5})TiO_3\text{-}(Bi_{0.5}\ K_{0.5})TiO_3$ systems. Jpn J Appl Phys 1999;38(9S):5564.

[38] Takenaka T, Maruyama K-I, Sakata K. $(Bi_{1/2}\ Na_{1/2})TiO_3\text{-}BaTiO_3$ system for lead-free piezoelectric ceramics. Jpn J Appl Phys 1991;30(9B):2236−9.

[39] Ma C, Guo H, Beckman SP, Tan X. Creation and destruction of morphotropic phase boundaries through electrical poling: a case study of lead-free $(Bi_{1/2}\ Na_{1/2})TiO_3\text{-}BaTiO_3$ piezoelectrics. Phys Rev Lett 2012;109(10).

[40] Ma C, Tan X. In situ transmission electron microscopy study on the phase transitions in lead-free $(1-x)(Bi_{1/2}\ Na_{1/2})\ TiO_3\text{-}xBaTiO_3$ ceramics. J Am Ceram Soc 2011;94(11):4040−4.

[41] Sapper E, Schaab S, Jo W, Granzow T, Rödel J. Influence of electric Fields on the depolarization temperature of Mn-doped $(1-x)Bi_{1/2}\ Na_{1/2}\ TiO_3\text{-}xBaTiO_3$. J Appl Phys 2012;111(1):014105.

[42] Sapper E, Novak N, Jo W, Granzow T, Rödel J. Electric-field-temperature phase diagram of the ferroelectric relaxor system $(1-x)(Bi_{1/2}\ Na_{1/2})TiO_3\text{-}xBaTiO_3$ doped with manganese. J Appl Phys 2014;115(19):194104.

[43] Sapper E, Dittmer R, Damjanovic D, Erdem E, Keeble DJ, Jo W, et al. Aging in the relaxor and ferroelectric state of Fe-doped $(1-x)(Bi_{1/2}\ Na_{1/2})TiO_3\text{-}xBaTiO_3$ piezoelectric ceramics. J Appl Phys 2014;116(10):104102.

[44] Matsubara M, Yamaguchi T, Kikuta K, Hirano S-i. Sinterability and piezoelectric properties of $(K,Na)NbO_3$ ceramics with novel sintering aid. Jpn J Appl Phys 2004;43(10):7159−63.

[45] Matsubara M, Yamaguchi T, Kikuta K, Hirano S-i. Sintering and piezoelectric properties of potassium sodium niobate ceramics with newly developed sintering aid. Jpn J Appl Phys 2005;44(1A): 258−63.

[46] Park H-Y, Seo I-T, Choi M-K, Nahm S, Lee H-G, Kang H-W, et al. Microstructure and piezoelectric properties of the CuO-added $(Na_{0.5}\ K_{0.5})\ (Nb_{0.97}\ Sb_{0.03}\ )\ O_3$ lead-free piezoelectric ceramics. J Appl Phys 2008;104(3):034103.

[47] Lim JB, Zhang S, Jeon J-H, Shrout TR. $(K,Na)NbO_3$-Based ceramics for piezoelectric “hard” lead-free material. J Am Ceram Soc 2010;93(5):1218−20.

[48] Tsai C-C, Chen S-F, Chu S-Y, Cheng CM, Kuan MC. The characteristics of ultrasonic therapeutic transducers and used lead-free non-stoichiometric NKN-based piezoelectric ceramics. Jpn J Appl Phys 2005;44(1A):258−63.

[49] Haertling GH. Ferroelectric ceramics: history and technology. J Am Ceram Soc 1999;82(4):797−818.

[50] Voigt W. Lehrbuch der kristallphysik (mit ausschluss der kristalloptik). Springer-Verlag; 1910.

[51] Jaffe H. Piezoelectric ceramics. J Am Ceram Soc 1958;41(11):494−8.

[52] Megaw HD. Origin of ferroelectricity in barium titanate and other perovskite-type crystals. Acta Crystallogr 1952;5(6):739−49.

[53] Sharpe CB, Brockus CG. Method for measuring the dielectric constant of ferroelectric ceramics at S-band frequencies. J Am Ceram Soc 1960;43(6):302−5.

[54] Merz WJ. The electric and optical behavior of $BaTiO_3$ single-domain crystals. Phys Rev 1949;76(8):1221−5.

[55] Merz WJ. Double hysteresis loop of $BaTiO_3$ at the curie point. Phys Rev 1953;91(3):513−7.

[56] Wieder HH. Ferroelectric hysteresis in barium titanate single crystals. J Appl Phys 1955;26(12):1479.

[57] Berlincourt D. Recent developments in ferroelectric transducer materials. Trans Ultrason Eng 1956:53−65.

[58] Perls TA, Diesel TJ, Dobrov WI. Primary pyroelectricity in barium titanate ceramics. J Appl Phys 1958;29(9):1297.

[59] Scott JF. Applications of modern ferroelectrics. Science 2007;315(5814):954−9.

[60] Damjanovic D. A morphotropic phase boundary system based on polarization rotation and polarization extension. Appl Phys Lett 2010;97(6):062906.

[61] Fu H, Cohen RE. Polarization rotation mechanism for ultrahigh electromechanical response in single-crystal piezoelectrics. Nature 2000;403(6767):281−3.

[62] Wada S, Suzuki S, Noma T, Suzuki T, Osada M, Kakihana M, et al. Enhanced piezoelectric property of barium titanate single crystals with engineered domain configurations. Jap J Appl Phys 1999;38(9S):5505.

[63] Jo W, Daniels JE, Jones JL, Tan X, Thomas PA, Damjanovic D, et al. Evolving morphotropic phase boundary in lead-free (Bi$_{1/2}$ Na$_{1/2}$)TiO$_3$-BaTiO$_3$ piezoceramics. J Appl Phys 2011;109(1):014110.

[64] Sato Y, Hirayama T, Ikuhara Y. Monoclinic nanodomains in morphotropic phase boundary Pb(Mg$_{1/3}$ Nb$_{2/3}$)O$_3$-PbTiO$_3$. Appl Phys Lett 2014;104(8):082905.

[65] Noheda B, Cox DE. Bridging phases at the morphotropic boundaries of lead oxide solid solutions. Phase Transit 2006;79(1−2):5−20.

[66] Kreisel J, Noheda B, Dkhil B. Phase transitions and ferroelectrics: revival and the future in the field. Phase Transit 2009;82(9):633−61.

[67] Noheda B, Cox DE, Shirane G, Guo R, Jones B, Cross LE. Stability of the monoclinic phase in the ferroelectric perovskite PbZr$_{1-x}$ Ti$_x$O$_3$. Phys Rev B 2000;63(1).

[68] Schönau KA, Schmitt LA, Knapp M, Fuess H, Eichel R-A, Kungl H, et al. Nanodomain Structure of Pb(Zr$_{1-x}$ Ti$_x$)O$_3$ at Its Morphotropic Phase Boundary: Investigations from local to average structure. Phys Rev B 2007;75(18).

[69] Pandey D, Singh AK, Baik S. Stability of ferroic phases in the highly piezoelectric Pb(Zr$_x$Ti$_{1-x}$)O$_3$ ceramics. Acta Crystallogr A 2008;64(Pt 1):192−203.

[70] Singh AK, Pandey D, Yoon SH, Baik S, Shin NS. High-resolution synchrotron x-ray diffraction study of Zr-rich compositions of Pb(Zr$_x$Ti$_{1-x}$)O$_3$ ($0.525 < x < 0.60$): evidence for the absence of the rhombohedral phase. Appl Phys Lett 2007;91(19):192904.

[71] Cordero F, Trequattrini F, Craciun F, Galassi C. Octahedral tilting, monoclinic phase and the phase diagram of PZT. J Phys C 2011;23(41):415901.

[72] Carreaud J, Kiat JM, Dkhil B, Algueró M, Ricote J, Jiménez R, et al. Monoclinic morphotropic phase and grain size-induced polarization rotation in Pb(Mg$_{1/3}$ Nb$_{2/3}$)O$_3$-PbTiO$_3$. Appl Phys Lett 2006;89(25):252906.

[73] Burkovsky RG, Bronwald YA, Filimonov AV, Rudskoy AI, Chernyshov D, Bosak A, et al. Structural heterogeneity and diffuse scattering in morphotropic lead zirconate-titanate single crystals. Phys Rev Lett 2012;109(9).

[74] Lummen TT, Gu Y, Wang J, Lei S, Xue F, Kumar A, et al. Thermotropic phase boundaries in classic ferroelectrics. Nat Commun 2014;5:3172.

[75] Schönau KA, Knapp M, Kungl H, Hoffmann MJ, Fuess H. In situ synchrotron diffraction investigation of morphotropic Pb(Zr$_{1-x}$ Ti$_x$)O$_3$ under an applied electric field. Phys Rev B 2007;76(14).

[76] Rossetti GA, Khachaturyan AG, Akcay G, Ni Y. Ferroelectric solid solutions with morphotropic Boundaries: vanishing polarization anisotropy, adaptive, polar glass, and two-phase states. J Appl Phys 2008;103(11):114113.

[77] Frantti J, Fujioka Y, Nieminen RM. Evidence against the polarization rotation model of piezoelectric perovskites at the morphotropic phase boundary. J Phys C 2008;20(47):472203.

[78] Janolin PE, Bouvier P, Kreisel J, Thomas PA, Kornev IA, Bellaiche L, et al. High-pressure effect on PbTiO$_3$: an investigation by Raman and X-Ray scattering up to 63 GPa. Phys Rev Lett 2008;101(23).

[79] Zhang Y, Xue D, Wu H, Ding X, Lookman T, Ren X. Adaptive ferroelectric state at morphotropic phase boundary: coexisting tetragonal and rhombohedral phases. Acta Mater 2014;71:176−84.

[80] Heitmann AA, Rossetti GA. Thermodynamics of ferroelectric solid solutions with morphotropic phase boundaries. J Am Ceram Soc 2014;97(6):1661−85.

[81] Datta K, Gorfman S, Thomas PA. On the symmetry of the morphotropic phase boundary in ferroelectric BiScO$_3$-PbTiO$_3$ system. Appl Phys Lett 2009;95(25):251901.

[82] Khachaturyan AG. Ferroelectric solid solutions with morphotropic boundary: rotational instability of polarization, metastable coexistence of phases and nanodomain adaptive states. Philos Mag 2010;90(1−4):37−60.

[83] Heitmann AA, Rossetti GA. Thermodynamics of polar anisotropy in morphotropic ferroelectric solid solutions. Philos Mag 2010;90(1−4):71−87.

[84] Schneider D, Jo W, Rödel J, Rytz D, Granzow T. Anisotropy of ferroelectric behavior of (1-x)Bi$_{1/2}$ Na$_{1/2}$ TiO$_3$-BaTiO$_3$ single crystals across the morphotropic phase boundary. J Appl Phys 2014;116(4):044111.

[85] Tennery VJ, Hang KW. Thermal and X-ray diffraction studies of NaNbO$_3$-KNbO$_3$ System. J Appl Phys 1968;39(10):4749−53.

[86] Dai YJ, Zhang XW, Chen KP. Morphotropic phase boundary and electrical properties of K$_{1-x}$ Na$_x$NbO$_3$ lead-free ceramics. Appl Phys Lett 2009;94(4):042905.

[87] Egerton L, Dillon DM. Piezoelectric and dielectric properties of ceramics in the system potassium-sodium niobate. J Am Ceram Soc 1959;42(9):438−42.

[88] Guo Y, Kakimoto K, Osato H. (Na$_{0.5}$ K$_{0.5}$ NbO$_3$-LiTaO$_3$ lead-free piezoelectric ceramics. Mater Lett 2005;59(2−3):241−4.

[89] Rubio-Marcos F, Ochoa P, Fernandez JF. Sintering and properties of lead-free (K,Na,Li)(Nb,Ta,Sb)O$_3$ ceramics. J Eur Ceram Soc 2007;27(13−15):4125−9.

[90] Zhang S-T, Kounga AB, Aulbach E, Ehrenberg H, Rödel J. Giant strain in lead-free piezoceramics Bi$_{0.5}$ Na$_{0.5}$ TiO$_3$-BaTiO$_3$-K$_{0.5}$ Na$_{0.5}$ NbO$_3$ system. Appl Phys Lett 2007;91(11):112906.

[91] Yang ZP, Chang YF, Wei LL. Phase transitional behavior and electrical properties of lead-free (K$_{0.44}$ Na$_{0.52}$ Li$_{0.04}$)(Nb$_{0.96-x}$ Ta$_x$Sb$_{0.04}$)O$_3$ piezoelectric ceramics. Appl Phys Lett 2007;90(4):042911.

[92] Hollenstein E, Davis M, Damjanovic D, Setter N. Piezoelectric properties of Li- and Ta-modified (K$_{0.5}$ Na$_{0.5}$)NbO$_3$ ceramics. Appl Phys Lett 2005;87(18):182905.

[93] Zhao P, Zhang BP, Li JF. Enhanced dielectric and piezoelectric properties in LiTaO$_3$-doped lead-free (K,Na)NbO$_3$ ceramics by optimizing sintering temperature. Scr Mater 2008;58(6):429−32.

[94] Wang K, Li JF. Domain engineering of lead-free Li-modified (K,Na) NbO$_3$ polycrystals with highly enhanced piezoelectricity. Adv Funct Mater 2010;20(12):1924−9.

[95] Shen ZY, Li YM, Jiang L, Li RR, Wang ZM, Hong Y, et al. Phase transition and electrical properties of LiNbO$_3$-modified K$_{0.49}$ Na$_{0.51}$ NbO$_3$ lead-free piezoceramics. J Mater Sci 2011;22(8):1071−5.

[96] Wang K, Li JF, Liu N. Phase transition and electrical properties of LiNbO$_3$-modified K$_{0.49}$ Na$_{0.51}$ NbO$_3$ lead-free piezoceramics. Appl Phys Lett 2008;93(9):092904.

[97] Wongsaenmai S, Ananta S, Yimnirun R. Effect of Li addition on phase formation behavior and electrical properties of (K$_{0.5}$ Na$_{0.5}$)NbO$_3$ lead free ceramics. Ceram Int 2012;38(1):147−52.

[98] Du H, Tang F, Liu D, Zhu D, Zhou W, Qu S. The microstructure and ferroelectric properties of (K$_{0.5}$ Na$_{0.5}$)NbO$_3$-LiNbO$_3$ lead-free piezoelectric ceramics. Mater Sci Eng 2007;136(2−3):165−9.

[99] Song HC, Cho KH, Park HY, Ahn CW, Nahm S, Uchino K, et al. Microstructure and piezoelectric properties of ($1-x$)(Na$_{0.5}$ K$_{0.5}$)NbO$_3$-xLiNbO$_3$ ceramics. J Am Ceram Soc 2007;90(6):1812−6.

[100] Klein N, Hollenstein E, Damjanovic D, Trodahl HJ, Setter N, Kuball M. A study of the phase diagram of (K,Na,Li)NbO$_3$ determined by dielectric and piezoelectric measurements, and Raman spectroscopy. J Appl Phys 2007;102(1):014112.

[101] Wang K, Li JF, Zhou J. High piezoelectric d$_{33}$ coefficient in Li-modified lead-free (Na,K)NbO$_3$ ceramics sintered at optimal temperature. Appl Phys Express 2011;4(6):061501.

[102] Wu J, Wang Y, Xiao D, Zhu J, Yu P, Wu L, et al. Piezoelectric properties of LiSbO$_3$-modified (K$_{0.48}$ Na$_{0.52}$)NbO$_3$ lead-free ceramics. Jpn J Appl Phys 2007;46(11):7375−7.

[103] Lin DM, Kwok KW, Lam KH, Chan HLW. Structure and electrical properties of K$_{0.5}$ Na$_{0.5}$ NbO$_3$-LiSbO$_3$ lead-free piezoelectric ceramics. J Appl Phys 2007;101(7):074111.

[104] Wu JG, Xiao D, Wang Y, Zhu J, Yu P, Jiang Y. Compositional dependence of phase structure and electrical properties in (K$_{0.42}$ Na$_{0.58}$)NbO$_3$-LiSbO$_3$ lead-free ceramics. J Appl Phys 2007;102(11):114113.

[105] Zang GZ, Wang JF, Chen HC, Su WB, Wang CM, Qi P, et al. Perovskite (Na$_{0.5}$ K$_{0.5}$)$_{1-x}$(LiSb)$_x$Nb$_{1-x}$ O$_3$ lead-free piezoceramics. Appl Phys Lett 2006;88(21):212908.

[106] Li H, Shih WY, Shih WH. Effect of antimony concentration on the crystalline structure, dielectric, and piezoelectric properties of $(Na_{0.5} K_{0.5})_{0.945} Li_{0.055} Nb_{1-x} Sb_xO_3$ solid solutions. J Am Ceram Soc 2007;90(10):3070−2.

[107] Zhang JL, Zong XJ, Wu L, Gao Y, Zheng P, Shao SF. Polymorphic phase transition and excellent piezoelectric performance of $(K_{0.55} Na_{0.45})_{0.965} Li_{0.035} Nb_{0.80} Ta_{0.20} O_3$ lead-free ceramics. Appl Phys Lett 2009;95(2):022909.

[108] Zhao P, Tu R, Goto T, Zhang BP, Yang S. Effect of Ta content on phase structure and electrical properties of piezoelectric lead-free $[(Na_{0.535} K_{0.480})_{0.942} Li_{0.058}](Nb_{1-x} Ta_x)O_3$ ceramics. J Am Ceram Soc 2008;91(10):3440−3.

[109] Kim MR, Song HC, Choi JW, Cho YS, Kim HJ, Yoon SJ. Synthesis and piezoelectric properties of $(1-x)(Na_{0.5} K_{0.5})NbO_3$-$x(Ba_{0.95} Sr_{0.05})TiO_3$ ceramics. J Electroceram 2009;23(2):502−5.

[110] Bafandeh MR, Gharahkhani R, Abbasi MH, Saidi A, Lee J-S, Han H-S. Improvement of piezoelectric and ferroelectric properties in (K, Na) NbO_3-based ceramics via microwave sintering. J Electroceram 2014;33(1−2):128−33.

[111] Moon SH, Choi JH, Chae KW, Kim JS, Cheon CI. The effect of pre-annealing on the microstructure of $(K,Na)NbO_3$ ceramics. Ceram Int 2013;39(3):2431−6.

[112] Kim JS, Lim SY, Ryu GH, Hussain A, Song TK, Park TG, et al. Effect of Na excess on the dielectric and piezoelectric properties of $(Na_{0.53} K_{0.47})(Nb_{0.55} Ta_{0.45})O_3$ ceramics. Phys Status Solidi A 2014;211(8):1715−9.

[113] Wang K, Yao F-Z, Jo W, Gobeljic D, Shvartsman VV, Lupascu DC, et al. Temperature-insensitive $(K,Na)NbO_3$-Based lead-free piezoactuator ceramics. Adv Funct Mater 2013;23(33):4079−86.

[114] Zhang SJ, Xia R, Shrout TR. Modified $(K_{0.5} Na_{0.5})NbO_3$ based lead-free piezoelectrics with broad temperature usage range. Appl Phys Lett 2007;91(13):132913.

[115] Wu J, Xiao D, Wang Y, Wu W, Zhang B, Li J, et al. $CaTiO_3$-Modified $[(K_{0.5} Na_{0.5})0.94Li_{0.06}](Nb_{0.94} Sb_{0.06})O_3$ lead-free piezoelectric ceramics with improved temperature stability. Scr Mater 2008;59(7):750−2.

[116] Wu J, Xiao D, Wang Y, Wu W, Zhang B, Zhu J, et al. Microstructure and electrical properties of (Li, Ag, Ta, Sb)-modified $(K_{0.50} Na_{0.50}) NbO_3$ lead-free ceramics with good temperature stability. J Phys D Appl Phys 2008;41(12):125405.

[117] Wang R, Bando H, Katsumata T, Inaguma Y, Taniguchi H, Mitsuru I. Tuning the Orthorhombic− rhombohedral phase transition temperature in sodium potassium niobate by incorporating barium zirconate. Phys Status Solidi (RRL) 2009;3(5):142−4.

[118] Liang W, Wu W, Xiao D, Zhu J. Effect of the addition of $CaZrO_3$ and $LiNbO_3$ on the phase transitions and piezoelectric properties of $K_{0.5} Na_{0.5} NbO_3$ lead-free ceramics. J Am Ceram Soc 2011;94(12):4317−22.

[119] Karaki T, Katayama T, Yoshida K, Maruyama S, Adachi M. Morphotropic phase boundary slope of $(K,Na,Li)NbO_3$-$BaZrO_3$ binary system adjusted using third component $(Bi,Na)TiO_3$ additive. Jpn J Appl Phys 2013;52(9S1):09KD11.

[120] Liang W, Wu W, Xiao D, Zhu J, Wu J. Construction of new morphotropic phase boundary in $0.94(K_{0.42-x} Na_{0.6} Ba_xNb_{1-x} Zr_x)O_3$-$0.06LiSbO_3$ lead-free piezoelectric ceramics. J Mater Sci 2011;46(21):6771−876.

[121] Wang R, Bando H, Kidate M, Nishihara Y, Itoh M. Effects of A-site ions on the phase transition temperatures and dielectric properties of $(1-x)(Na_{0.5} K_{0.5})NbO_3$-$xAZrO_3$ solid solutions. Jpn J Appl Phys 2011;50(9S2):09ND10.

[122] Liang W, Wu W, Xiao D, Zhu J, Zhu J, Wu J. New crystallographic dielectric phase boundary in $K_{0.5} Na_{0.5} NbO_3$-based lead-free ceramics. Phys Status Solidi (RRL) 2011;5(7):220−2.

[123] Zuo R, Fu J. Rhombohedral−tetragonal phase coexistence and piezoelectric properties of $(NaK)(NbSb)O_3$-$LiTaO_3$-$BaZrO_3$ lead-free ceramics. J Am Ceram Soc 2011;94(5):1467−70.

[124] Wang X, Wu J, Cheng X, Zhang B, Xiao D, Zhu J, et al. Rhombohedral-tetragonal phase boundary and electrical properties of new $K_{0.48} Na_{0.52} Nb_{0.98} Sb_{0.02} O_3$-$Bi_{0.5} Na_{0.5} ZrO_3$ lead-free piezoceramics. J Phys D Appl Phys 2013;46(49):495305.

[125] Huang T, Xiao D, Liu C, Li F, Wu B, Wu J, et al. Effect of $SrZrO_3$ on phase structure and electrical properties of $0.974(K_{0.5} Na_{0.5}) NbO_3$-$0.026Bi_{0.5} K_{0.5} TiO_3$ lead-free ceramics. Ceram Int 2013;40(2):2731−5.

[126] Liu C, Xiao D, Huang T, Wu J, Li F, Wu B, et al. Composition induced Rhombohedral−Tetragonal phase boundary in $BaZrO_3$ modified $(K_{0.445} Na_{0.50} Li_{0.055})NbO_3$ lead-free ceramics. Matter Lett 2014;120(1):275−8.

[127] Cheng X, Gou Q, Wu J, Wang X, Zhang B, Xiao D, et al. Dielectric, ferroelectric, and piezoelectric properties in potassium sodium niobate ceramics with rhombohedral-orthorhombic and orthorhombic-tetragonal phase boundaries. Ceram Int 2014;40(4):5771−9.

[128] Li Y-M, Shen Z-Y, Wu F, Pan T-Z, Wang Z-M, Xiao Z-G. Enhancement of piezoelectric properties and temperature stability by forming an MPB in KNN-based lead-free ceramics. J Mater Sci Mater Electron 2014;25(2):1028−32.

[129] Wang X, Wu J, Xiao D, Zhu J, Cheng X, Zheng T, et al. Giant piezoelectricity in potassium-sodium niobate lead-free ceramics. J Am Chem Soc 2014;136(7):2905−10.

[130] Wu J, Xiao J, Zheng T, Wang X, Cheng X, Zhang B, et al. Giant piezoelectricity of $(K,Na)(Nb,Sb)O_3$-$(Bi,Na, K,Pb)ZrO_3$ ceramics with rhombohedral-tetragonal (R-T) phase boundary. Scr Mater 2014;88(1):41−4.

[131] Wang H, Wu J, Cheng X, Xiao D, Zhu J. New phase boundary and piezoelectric properties in (K, Na)NbO_3 based ceramics. J Alloys Compd 2014;585(5):748−52.

[132] Cheng X, Wu J, Zheng T, Wang X, Zhang B, Xiao D, et al. Rhombohedral-tetragonal phase coexistence and piezoelectric properties based on potassium-sodium niobate ternary system. J Alloys Compd 2014;610(15):86−91.

[133] Wang R, Wang K, Yao F, Li J-F, Schader FH, Webber KG, et al. Temperature stability of lead-free niobate piezoceramics with engineered morphotropic phase boundary. J Am Ceram Soc 2015;98(7):2177−82.

[134] Vig JR. Quartz Crystal resonators and oscillators for frequency control and timing applications − a tutorial. 2001. http://www.ieee-uffc.org/frequency-control/learning-vig-tut.asp. AD-M001251.

[135] Uchino K. Introduction to piezoelectric actuators and transducers. In: International Conference on Intelligent Materials (5th). Smart Systems & Nanotechnology; 2003. p. 1−40.

[136] Raymond MV, Smyth DM. Defects and charge transport in perovskite ferroelectrics. J Phys Chem Solids 1996;57(10):1507−11.

[137] Smyth DM. Defects and order in perovskite-related oxides. Ann Rev Mater Sci 1985;15(1):329−57.

[138] Ren X. Large electric-field-induced strain in ferroelectric crystals by point-defect-mediated reversible domain switching. Nat Mater 2004;3(2):91−4.

[139] Granzow T, Suvaci E, Kungl H, Hoffmann MJ. Deaging of heat-treated iron-doped lead zirconate titanate ceramics. Appl Phys Lett 2006;89(26):262908.

[140] Eichel R-A, Erhart P, Träskelin P, Albe K, Kungl H, Hoffmann M. Defect-dipole formation in copper-doped $PbTiO_3$ ferroelectrics. Phys Rev Lett 2008;100(9):095504.

[141] Erhart P, Eichel RA, Träskelin P, Albe K. Association of oxygen vacancies with impurity metal ions in Lead titanate. Phys Rev B 2007;76(17):174116.

[142] Carl K, Hardtl KH. Electrical after-effects in Pb(Ti, Zr)O_3 ceramics. Ferroelectrics 1977;17(1):473−86.

[143] Arlt G, Neumann H. Internal bias in ferroelectric ceramics: origin and time dependence. Ferroelectrics 1988;87(1):109−20.

[144] Hall DA, Stevenson PJ. Field-induced destabilisation of hard PZT ceramics. Ferroelectrics 1996;187(1):23−37.

[145] Ren X, Zhang LX. Electro-shape-memory effect in ferroelectric martensite. Mater Sci Eng A 2006;438−440:1071−6.

[146] Eichel RA, Erunal E, Drahus MD, Smyth DM, van Tol J, Acker J, et al. Local variations in defect polarization and covalent bonding in

ferroelectric Cu^{2+}-doped PZT and KNN functional ceramics at the morphotropic phase boundary. Phys Chem Chem Phys 2009;11(39):8698−705.

[147] Park H-Y, Ahn C-W, Song H-C, Lee J-H, Nahm S, Uchino K, et al. Microstructure and piezoelectric properties of $0.95(Na_{0.5}\ K_{0.5})NbO_3$-$0.05BaTiO_3$ ceramics. Appl Phys Lett 2006;89(6):062906.

[148] Gao D, Kwok KW, Lin D, Chan HLW. Microstructure and electrical properties of La-modified $K_{0.5}\ Na_{0.5}\ NbO_3$ lead-free piezoelectric ceramics. J Phys D 2009;42(3):035411.

[149] Rödel J, Jo W, Seifert KTP, Anton E-M, Granzow T, Damjanovic D. Perspective on the development of lead-free Piezoceramics. J Am Ceram Soc 2009;92(6):1153−77.

[150] Herabut A, Safari A. Processing and electromechanical properties of $(Bi_{0.5}\ Na_{0.5})_{(1-1.5x)}La_xTiO_3$ ceramics. J Am Ceram Soc 1997;80(11):2954−8.

[151] Li J, Wang F, Leung CM, Or SW, Tang Y, Chen X, et al. Large strain response in acceptor- and donor-doped $Bi_{0.5}\ Na_{0.5}\ TiO_3$-based lead-free ceramics. J Mater Sci 2011;46(17):5702−8.

[152] Jo W, Erdem E, Eichel R-A, Glaum J, Granzow T, Damjanovic D, et al. Effect of Nb-donor and Fe-acceptor dopants in $(Bi_{1/2}\ Na_{1/2})TiO_3$-$BaTiO_3$-$(K_{0.5}\ Na_{0.5})NbO_3$ lead-free piezoceramics. J Appl Phys 2010;108(1):014110.

[153] Jo W, Ollagnier J-B, Park J-L, Anton E-M, Kwon O-J, Park C, et al. CuO as a sintering additive for $(Bi_{1/2}\ Na_{1/2})TiO_3$-$BaTiO_3$-$(K_{0.5}\ Na_{0.5})NbO_3$ lead-free piezoceramics. J Eur Ceram Soc 2011;31(12):2107−17.

[154] Aksel E, Erdem E, Jakes P, Jones JL, Eichel R-A. Defect structure and materials 'Hardening' in $Fe_2\ O_3$-doped $(Bi_{0.5}\ Na_{0.5})TiO_3$ ferroelectrics. Appl Phys Lett 2010;97(1):012903.

[155] Roberts S. Dielectric properties of Lead zirconate and barium-lead zirconate. J Am Ceram Soc 1950;33(2):63−6.

[156] Sawaguchi E, Mitsuma T, Ishii Z. Double hysteresis loop of $(Pb_\lambda Ca_{1-\lambda})TiO_3$ ceramics. J Phys Soc Jpn 1956;11(12). 1298−1298.

[157] Nomura S, Sawada S. Dielectric properties of lead strontium titanate. J Phys Soc Jpn 1955;10(2):108−11.

[158] Shirane G. Ferroelectricity and antiferroelectricity in ceramic $PbZrO_3$ containing Ba or Sr. Phys Rev 1952;86(2):219−27.

[159] Shirane G, Hoshino S. Crystal structure of the ferroelectric phase in $PbZrO_3$ containing Ba or Ti. Phys Rev 1952;86(2):248−9.

[160] Tennery VJ. A study of the phase transitions in $PbZrO_3$. J Electrochem Soc 1965;112(11):1117−20.

[161] Tennery VJ. High-temperature phase transitions in $PbZrO_3$. J Am Ceram Soc 1966;49(9):483−6.

[162] Sawaguchi E. Ferroelectricity versus antiferroelectricity in the solid solutions of $PbZrO_3$ and $PbTiO_3$. J Phys Soc Jpn 1953;8(5):615−29.

[163] Marutake M, Ikeda T. Elastic properties of Lead zirconate. J Phys Soc Jpn 1955;10(6):424−8.

[164] Shirane G, Pepinsky R. Phase transitions in antiferroelectric $PbHfO_3$. Phys Rev 1953;91:812−5.

[165] Ikeda T. A few quaternary systems of perovskite type $A^{2+}\ B^{4+}\ O_3$ solid solutions. J Phys Soc Jpn 1959;14(10):1286−94.

[166] Jaffe B, Roth R, Marzullo S. Properties of piezoelectric ceramics in the solid-solution series lead titanate-lead zirconate-lead oxide: tin oxide and lead titanate-lead hafnate. J Res Natl Bur Stand 1955;55(5):239−54.

[167] Arlt G, Hennings D, De With G. Dielectric properties of fine-grained barium titanate ceramics. J Appl Phys 1985;58(4):1619−25.

[168] Uchino K, Sadanaga E, Hirose T. Dependence of the crystal structure on particle size in barium titanate. J Am Ceram Soc 1989;72(8):1555.

[169] Darlington CNW, Cernik RJ. The effects of isovalent and non-isovalent impurities on the ferroelectric phase transition in barium titanate. J Phys Condens Matter 1993;5(32):5963.

[170] Heaney PJ. Phase transformations induced by solid solution. Rev Mineral Geochem 2000;39(1):135−74.

[171] Soon HP, Wang J. Ferroelectric crossovers triggered by isovalent A-site substitution in $Pb_{0.7}\ La_{0.2}\ TiO_3$. J Appl Phys 1993;100(12):124101.

[172] Devidas G, Prakash G. Dielectric properties of A-and B-site doped $BaTiO_3$: effect of La and Ga. Phys B Condens Matter 2009;404(12):1799−805.

[173] Nomura S. Dielectric properties of titanates containg Sn^{4+} ions I. J Phys Soc Jpn 1955;10(2):112−9.

[174] Shvartsman VV, Dec J, Xu ZK, Banys J, Keburis P, Kleemann W. Crossover from ferroelectric to relaxor behavior in $BaTi\ Sn_xO_3$ solid solutions. Phase Transit 2008;81(11−12):1013−21.

[175] Mitsui T, Westphal WB. Dielectric and X-Ray studies of $Ca_xBa_{1-x}\ TiO_3$ and $Ca_xSr_{1-x}\ TiO_3$. Phys Rev 1961;124(5):1354−9.

[176] Rushman DF, Strivens MA. The permittivity of polycrystals of the perovskite type. Trans Faraday Soc 1946;42. A231−A223.

[177] Shirane G, Suzuki K. On the phase transition in barium-lead titanate (1). J Phys Soc Jpn 1951;6(4):274−8.

[178] Shirane G, Hoshino S, Suzuki K. Crystal structure of lead titanate and of lead-barium titanate. J Phys Soc Jpn 1950;5(6):453−5.

[179] Jackson W, Reddish W. High permittivity crystalline aggregates. Nature 1945;156(3972):717.

[180] Shirane G, Takeda A. Volume change at three transitions in $BaTiO_3$ ceramics. J Phys Soc Jpn 1951;6(2):128−9.

[181] Weaver HE. Dielectric properties of single crystals of $SrTiO_3$ at low temperatures. Phys Chem Solids 1959;11(3):274−7.

[182] Edwin BJ. Poltcrystalline Ceramic Material, US Patent 2,708,243 (1955).

[183] Hennings D, Schnell A, Simon G. Diffuse ferroelectric phase transitions in $Ba(Ti_{1-y}\ Zr_y)O_3$ ceramics. J Am Ceram Soc 1982;65(11):539−44.

[184] Jonker GH, Kwestroo W. The ternary systems BaO-TiO_2-SnO_2 and BaO-TiO_2-ZrO_2. J Phys Soc Jpn 1958;41(10):390−4.

[185] Payne WH, Tennery VJ. Dielectric and structural investigations of the system $BaTiO_3$-$BaHfO_3$. J Am Ceram Soc 1965;48(8):413−7.

[186] Jo W, Rödel J. Electric-field-induced volume change and room temperature phase stability of $(Bi_{1/2}\ Na_{1/2})TiO_3$-$x$ mol.% $BaTiO_3$ piezoceramics. Appl Phys Lett 2011;99(4):042901.

[187] Zhang S-T, Kounga AB, Aulbach E, Granzow T, Jo W, Kleebe H-J, et al. Lead-free piezoceramics with giant strain in the system $Bi_{0.5}\ Na_{0.5}\ TiO_3$-$BaTiO_3$-$K_{0.5}\ Na_{0.5}\ NbO_3$. I structure and room temperature properties. J Appl Phys 2008;103(3):034107.

[188] Zhang S-T, Kounga AB, Aulbach E, Jo W, Granzow T, Ehrenberg H, et al. Lead-free piezoceramics with giant strain in the system $Bi_{0.5}\ Na_{0.5}\ TiO_3$-$BaTiO_3$-$K_{0.5}\ Na_{0.5}\ NbO_3$. II temperature dependent properties. J Appl Phys 2008;103(3):034108.

[189] Han H-S, Jo W, Rödel J, Hong I-K, Tai W-P, Lee J-S. Coexistence of ergodicity and nonergodicity in $LaFeO_3$-modified $Bi_{1/2}(Na_{0.78}\ K_{0.22})_{1/2}\ TiO_3$ relaxors. J Phys Condens Matter 2012;24(36):365901.

[190] Han H-S, Jo W, Kang J-K, Ahn C-W, Kim W-I, Ahn K-K, et al. Incipient piezoelectrics and electrostriction behavior in Sn-doped $Bi_{1/2}(Na_{0.82}\ K_{0.18})_{1/2}\ TiO_3$ lead-free ceramics. J Appl Phys 2013;113(15):154102.

[191] Lee D-S, Jeong S-J, Kim M-S, Koh J-H. Electric field induced polarization and strain of Bi-based ceramic composites. J Appl Phys 2012;112(12):124109.

[192] Chiang Y-M, Farrey GW, Soukhojak AN. Lead-Free high-strain Single-Crystal piezoelectrics in the alkaline-bismuth-titanate perovskite family. Appl Phys Lett 1998;73:3683−5.

[193] Farrey GW, Soukhojak A, Sheets S, Chiang Y-M. Growth and characterization of $Na_{1/2}\ Bi_{1/2}\ TiO_3$-$K_{1/2}\ Bi_{1/2}\ TiO_3\ BaTiO_3$ single crystal piezoelectrics. In: Applications of ferroelectrics, 1998 ISAF 98 Proceedings of the Eleventh IEEE international Symposium on; 1998. p. 551−4.

[194] Jones GO, Thomas PA. Investigation of the structure and phase transitions in the novel A-site substituted distorted perovskite compound $Na_{0.5}\ Bi_{0.5}\ TiO_3$. Acta Cryst B 2002;58:168−78.

[195] Jones GO, Kreisel J, Thomas PA. A structural study of the $(Na_{1-x}\ K_x)_{0.5}\ Bi_{0.5}\ TiO_3$ perovskite series as a function of substitution (x) and temperature. Powder Diffr 2002;17:301−19.

[196] Jo W, Granzow T, Aulbach E, Rödel J, Damjanovic D. Origin of the large strain response in $(K_{0.5}\ Na_{0.5})NbO_3$-modified $(Bi_{0.5}\ Na_{0.5})TiO_3$-$BaTiO_3$ lead-free piezoceramics. J Appl Phys 2009;105(9):094102.

[197] Bell AJ. Calculations of dielectric properties from the superparaelectric model of relaxors. J Phys Condens Matter 1993;5(46):8773−92.

[198] Glazounov AE, Tagantsev AK, Bell AJ. Evidence for domain-type dynamics in the ergodic phase of the $PbMg_{1/3}$ $Nb_{2/3}$ O_3 relaxor ferroelectric. Phys Rev B 1996;53(17):11281.

[199] Jo W, Schaab S, Sapper E, Schmitt LA, Kleebe H-J, Bell AJ, et al. On the phase identity and its thermal evolution of lead-free $(Bi_{1/2}$ $Na_{1/2})$ TiO_3 $-$ 6 mol% $BaTiO_3$. J Appl Phys 2011;110(7):074106.

[200] Viehland D, Jang SJ, Cross LE, Wuttig M. Freezing of the polarization fluctuations in lead magnesium niobate relaxors. J Appl Phys 1990;68(6):2916—21.

[201] Viehland D, Wuttig M, Cross LE. The glassy behavior of relaxor ferroelectrics. Ferroelectrics 1991;120(1):71—7.

[202] Bobnar V, Kutnjak Z, Pirc R, Levstik A. Electric-field-temperature phase diagram of the relaxor ferroelectric lanthanum-modified lead zirconate titanate. Phys Rev B 1999;60(9):6420—7.

[203] Schaab S, Granzow T. Temperature dependent switching mechanism of $(Pb_{0.92}$ $La_{0.08})(Zr_{0.65}$ $Ti_{0.35})O_3$ investigated by small and large signal measurements. Appl Phys Lett 2010;97(13):132902.

[204] Park S-E, Pan M-J, Markowski K, Yoshikawa S, Cross LE. Electric field induced phase transition of antiferroelectric lead lanthanum zirconate titanate stannate ceramics. J Appl Phys 1997;82(4):1798—803.

[205] Wang K, Hussain A, Jo W, Rödel J. Temperature-dependent properties of $(Bi_{1/2}$ $Na_{1/2})TiO_3$-$(Bi_{1/2}$ $K_{1/2})TiO_3$-$SrTiO_3$ lead-free piezoceramics. J Am Ceram Soc 2012;95(7):2241—7.

[206] Seifert KTP, Jo W, Rödel J. Temperature-insensitive large strain of $(Bi_{1/2}$ $Na_{1/2})TiO_3$-$(Bi_{1/2}$ $K_{1/2})TiO_3$-$(K_{0.5}$ $Na_{0.5})NbO_3$ lead-free piezoceramics. J Am Ceram Soc 2010;93(5):1392—6.

[207] Luo Z, Glaum J, Granzow T, Jo W, Dittmer R, Hoffman M, et al. Bipolar and unipolar fatigue of ferroelectric BNT-based lead-free piezoceramics. J Am Ceram Soc 2011;94:529—35.

[208] Luo Z, Granzow T, Glaum J, Jo W, Rödel J, Hoffman M. Effect of ferroelectric long-range order on the unipolar and bipolar electric fatigue in $Bi_{1/2}$ $Na_{1/2}$ TiO_3-based lead-free piezoceramics. J Am Ceram Soc 2011;94:3927—33.

[209] Sapper E, Gassmann A, Gjødvad L, Jo W, Granzow T, Rödel J. Cycling stability of lead-free BNT-8BT and BNT-6BT-3KNN multilayer actuators and bulk ceramics. J Eur Ceram Soc 2014;34:653—61.

[210] Hiruma Y, Imai Y, Watanabe Y, Nagata H, Takenaka T. Large electrostrain near the phase transition temperature of $(Bi_{0.5}$ $Na_{0.5})TiO_3$-$SrTiO_3$ ferroelectric ceramics. Appl Phys Lett 2008;92(26):262904.

[211] Lee D-S, Lim D-H, Kim M-S, Kim K-H, Jeong S-J. Electric field-induced deformation behavior in mixed $Bi_{0.5}$ $Na_{0.5}$ TiO_3 and $Bi_{0.5}(Na_{0.75}$ $K_{0.25})_{0.5}$ TiO_3-$BiAlO_3$. Appl Phys Lett 2011;99(6):062906.

[212] Groh C, Franzbach DJ, Jo W, Webber KG, Kling J, Schmitt LA, et al. Relaxor/Ferroelectric composites: a solution in the quest for practically viable lead-free incipient piezoceramics. Adv Funct Mater 2014;24(3):356—62.

[213] Aman U, Ahn CW, Amir U, Kim IW. Large strain under a low electric field in lead-free bismuth-based piezoelectrics. Appl Phys Lett 2013;103(2):022906.

[214] Nguyen V-Q, Hong C, Lee H-Y, Kong Y-M, Lee J-S, Ahn KK. Enhancement in microstucture and stain properties of $Bi_{1/2}$ Ba, $K_{1/2}$ TiO_3-based lead-free ceramics by Li-subsitution. J Korean Phys Soc 2012;61(6):895—8.

[215] Dittmer R, Jo W, Daniels J, Schaab S, Rödel J. Relaxor characteristics of morphotropic phase boundary $(Bi_{1/2}$ $Na_{1/2})TiO_3$-$(Bi_{1/2}$ $K_{1/2})TiO_3$ modified with $Bi(Zn_{1/2}$ $Ti_{1/2})O_3$. J Am Ceram Soc 2011;94(12):4283—90.

[216] Cho J-H, Jeong Y-H, Nam J-H, Yun J-S, Park Y-J. Phase transition and piezoelectric properties of lead-free $(Bi_{1/2}$ $Na_{1/2})TiO_3$-$BaTiO_3$ ceramics. Ceram Int 2014;40(6):8419—25.

[217] Cho J-H, Jeon C-J, Lee K-T, Park J-S, Jeong Y-H, Yun J-S. Electric field induced polarization and strain of $(Bi_{1/2}$ $Na_{1/2})TiO_3$-$BaTiO_3$ ceramics. Ceram Int 2015;41(3):4789—97.

[218] Rahman JU, Hussain A, Maqbool A, Ryu GH, Song TK, Kim W-J, et al. Field induced strain response of lead-free $BaZrO_3$-modified $Bi_{0.5}$ Na $_{0.5}$ TiO_3-$BaTiO_3$ ceramics. J Alloys Compd 2014;593:97—102.

[219] Lee M-H, Kim D-J, Park J-S, Kim S-W, Song T-K, Kim M-H, et al. High-performance lead-free piezoceramics with high curie temperatures. Adv Mater 2015;27:6976—82.

[220] Rahman JU, Hussain A, Maqbool A, Malik RA, Song TK, Kim MH, et al. Effect of donor doping on the ferroelectric and the piezoelectric properties of lead-free $0.97(Bi_{0.5}$ $Na_{0.5}$ Ti_{1-x} $Nb_x)O_3$-0.03 $BaZrO_3$ ceramics. J Korean Phys Soc 2015;67(7):1240—5.

[221] Dinh TH, Bafandeh MR, Kang J-K, Hong C-H, Jo W, Lee JS. Comparison of structural, ferroelectric, and strain properties between A-site donor and acceptor doped $Bi_{1/2}(Na_{0.82}$ K $_{0.18})_{1/2}$ TiO_3 ceramics. Ceram Int 2015;41(1):S458—63.

[222] Nguyen V-Q, Han H-S, Kim K-J, Dang D-D, Ahn K-K, Lee J-S. Strain enhancement in $Bi_{1/2}(Na_{0.82}$ $K_{0.18})_{1/2}$ TiO_3 lead-free electromechanical ceramics by co-doping with Li and Ta. J Alloys Compd 2012;511(1):237—41.

[223] Lee J-S, Pham K-N, Han H-S, Lee H-B, Tran VDN. Strain enhancement of lead-free $Bi_{1/2}(Na_{0.82}$ $K_{0.18})_{1/2}$ TiO_3 ceramics by Sn doping. J Korean Phys Soc 2012;60(2):212—5.

[224] Han H-S, Ahn C-W, Kim I-W, Hussain A, Lee J-S. Destabilization of ferroelectric order in bismuth perovskite ceramics by A-site vacancies. Mater Lett 2012;70:98—100.

[225] Acosta M, Jo W, Rödel J. Temperature- and frequency-dependent properties of the $0.75Bi_{1/2}$ $Na_{1/2}$ TiO_3-$0.25SrTiO_3$ lead-free incipient piezoceramic. J Am Ceram Soc 2014;97:1937—43.

[226] Choi S-Y, Jeong S-J, Lee D-S, Kim M-S, Lee J-S, Cho JH, et al. Gigantic electrostrain in duplex structured alkaline niobates. Chem Mater 2012;24(17):3363—9.

[227] Lee D-S, Jeong S-J, Park E-C, Song J-S. Characteristic of grain oriented $(Bi_{0.5}$ $Na_{0.5})TiO_3$-$BaTiO_3$ ceramics. J Electroceram 2006;17(2—4):505—8.

[228] Dauman R. Bone conduction: an explanation for this phenomenon comprising complex mechanisms. Eur Ann Otorhinolaryngol Head Neck Dis 2013;130(4):209—13.

[229] Kim MJ. Terminal with a Piezoelectric Speaker System and Method for Operating thereof, US Patent App 14/014,554 (2014).

[230] Ok Y-P, Kang J-K, Hong C-H, Lee J-S. Viscosity sensor using piezoelectric ceramic resonators. Korean Inst Electr Electron Mater Eng 2012;25(5):361—5.

[231] Fähler S, Rößler UK, Kastner O, Eckert J, Eggeler G, Emmerich H, et al. Caloric effects in ferroic materials: new concepts for cooling. Adv Eng Mater 2012;14(1—2):10—9.

[232] Ditas P, Hennig E, Kynast A. Lead-Free piezoceramic materials for ultrasonic applications. In: Sensors and measuring systems 2014; 17 ITG/GMA Symposium; Proceedings of; 2014. p. 1—4.

[233] Hong C-H, Han H-S, Lee J-S, Wang K, Yao F-Z, Li J-F, et al. Ring-type rotary ultrasonic motor using lead-free ceramics. J Sens Sci Technol 2015;24(4):228—31.

[234] Tou T, Hamaguti Y, Maida Y, Yamamori H, Takahashi K, Terashima Y. Properties of $(Bi_{0.5}$ $Na_{0.5})TiO_3$-$BaTiO_3$-$(Bi_{0.5}$ $Na_{0.5})(Mn_{1/3}$ $Nb_{2/3})O_3$ lead-free piezoelectric ceramics and its application to ultrasonic cleaner. Jpn J Appl Phys 2009;48(7S):07GM03.

[235] Mathieson A, DeAngelis D. Feasibility of lead-free piezoceramic based power ultrasonic transducers. In: Ultrasonics Symposium (IUS), 2014 IEEE International; 2014. p. 2075—8.

[236] Harada S, Aoi K, Hirata T, Ito Y. Nonresonant Type Knock Sensor, US Patent 6,752,005 (2004).

[237] Kang J-K, Han H-S, Jeong S-K, Ahn K-K, Jeong S-J, Lee J-S. Microwave and conventional sintering of lead-free (K, Na) NbO_3-based piezoelectric ceramic multilayer actuators. J Ceram Process Res 2013;14(2):230—3.

[238] Nguyen V-Q, Kang J-K, Han H-S, Lee H-Y, Jeong S-J, Ahn C-W, et al. Bi-based lead-free ceramic multilayer actuators using AgPd-$(Na_{0.51}$ $K_{0.47}$ $Li_{0.02})(Nb_{0.8}$ $Ta_{0.2})O_3$ composite inner electrodes. Sens Actuat A Phys 2013;200:107—13.

[239] Han H-S, Park E-C, Lee J-S, Yoon JI, Ahn KK. Low-firing $Pb(Zr,Ti)O_3$-based multilayer ceramic actuators using Ag inner electrode. Trans Electr Electron Mater 2011;12(6):249—52.

Mr. Chang-Hyo Hong, Ulsan National Institute of Science and Technology (UNIST). Email: changhyo@unist.ac.kr. Chang-Hyo Hong is currently a Ph. D. course candidate under supervision of Prof. Wook Jo at School of Materials Science and Engineering, Ulsan National Institute of Science and Technology (UNIST), Ulsan, Korea. His research interests are mainly on fundamental analysis of relaxors and lead-free piezoceramics.

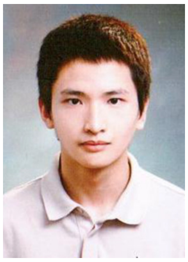

Mr. Hwang-Pill Kim, Ulsan National Institute of Science and Technology (UNIST). Email: pollux234@unist.ac.kr. Hwang-Pill Kim is currently a combined MS/Ph.D. candidate in Materials Science and Engineering at Ulsan National Institute of Science and Technology (UNIST), Republic of Korea. He got his B.S degree in Material Science and Engineering in 2015 from UNIST. His research field is about the engineering of ferroelectric domain structures under the supervision of Prof. Wook Jo.

Mr. Byung-Yul Choi, Ulsan National Institute of Science and Technology (UNIST). Email: bychoi@unist.ac.kr. Byung-Yul Choi is a candidate of the combined master and doctorial course in the UNIST Graduate School of Material Science and Engineering. He received the B.S. degree from the Inha University, Incheon, Korea, in 2002. From 2002 to 2008, he had been a Researcher at the Advanced Materials & Science Division, Korea Institute of Ceramic Engineering and Technology (KICET). And he had worked in the R&D center, Innochips, Co. Ltd. from 2008 to 2014 as a Senior Engineer and Project Leader. His research fields are the Piezoelectric actuator and sensor systems for practical applications, Ultrasonic devices and Device simulation/modeling, etc.

Dr. Hyoung-Su Han, Ulsan National Institute of Science and Technology (UNIST). Email: hshan@unist.ac.kr. Dr. Hyoung-Su Han is currently a postdoctoral research associate at Professor Wook Jo's group in UNIST, Ulsan, Korea. He received his B.S. degree (2008), M.S. dgree (2010), and Ph.D. degree (2013) from University of Ulsan. He had worked as a postdoctoral associate at the Technische Universität Darmstadt from 2014 to 2015. His recent research focuses on BNT-based lead-free relaxors, KNN-based lead-free piezoelectric materials, and the processing of the multilayer ceramic actuator (MLAs).

Prof. Jae Sung Son, Ulsan National Institute of Science and Technology (UNIST). Email: jsson@unist.ac.kr. Dr. Jae Sung Son received his B.S. (2005) in School of Chemical and Biological Engineering and Ph.D. (2011) in Interdisciplinary of Nanoscience and Technology from Seoul National University (SNU) in Korea under the supervision of Prof. Taeghwan Hyeon. During his doctorate period, he has focused on the development of the synthesis of semiconductor 2D nanomaterials and thermoelectric applications of Bi and Bi_2Te_3 nanostructures. After his postdoctoral training at University of Chicago under the supervision of Prof. Dmitri Talapin in USA, he joined the School of Materials Science and Engineering of Ulsan National Institute of Science and Technology (UNIST) in 2014. Now he is focusing on the synthesis of functional nanomaterials and inorganic molecular ions for ligands or solders of nanomaterials, and their synergetic combinations for new-typed energy and electronic devices with high performances.

Dr. Chang Won Ahn, University of Ulsan. Email: cwahn@ulsan.ac.kr, cwahn74@gmail.com. Dr. Chang Won Ahn is a Research Professor in Department of Physics and Energy Harvest Storage Research Center (EHSRC) at University of Ulsan, Republic of Korea. He received his Ph.D. from University of Ulsan in Department of Physics in 2007. His recent research interest is focused on the synthesis of nanotubes, thin films and textured ceramics of lead-free piezoelectric materials for the applications of energy-conversion devices. Particular interests are photovoltaic and photocatalysis effects of nanoporous ferroelectric materials. He has published over 110 papers in international journals and holds 10 Korean patents.

Prof. Wook Jo, Ulsan National Institute of Science and Technology (UNIST). Email: wookjo@unist.ac.kr. Dr. Wook Jo is a Professor at the School of Materials Science and Engineering, Ulsan National Institute of Science and Technology (UNIST), Ulsan, Korea. Prior to joining the faculty of UNIST in 2014, he had served as a group leader for the Processing of Ferroelectrics lab at the Institute of Materials Science, Technische Universität Darmstadt, Germany as of 2007. His recent research focuses on the functional properties of ferroelectric materials with a special emphasis on the lead-free piezoceramics and relaxor ferroelectrics. He has published over 120 papers in refereed international journals and 6 books, and holds 6 patents.